

Two photons into $\pi^0\pi^0$

J. A. Oller, L. Roca

Departamento de Física. Universidad de Murcia. E-30071, Murcia. Spain.
oller@um.es , luisroca@um.es

Abstract

We perform a theoretical study based on dispersion relations of the reaction $\gamma\gamma \rightarrow \pi^0\pi^0$ emphasizing the low energy region. We discuss how the $f_0(980)$ signal emerges in $\gamma\gamma \rightarrow \pi\pi$ within the dispersive approach and how this fixes to a large extent the phase of the isoscalar S-wave $\gamma\gamma \rightarrow \pi\pi$ amplitude above the $K\bar{K}$ threshold. This allows us to make sharper predictions for the cross section at lower energies and our results could then be used to distinguish between different $\pi\pi$ isoscalar S-wave parameterizations with the advent of new precise data on $\gamma\gamma \rightarrow \pi^0\pi^0$. We compare our dispersive approach with an updated calculation employing Unitary Chiral Perturbation Theory (U χ PT). We also pay special attention to the role played by the σ resonance in $\gamma\gamma \rightarrow \pi\pi$ and calculate its coupling and width to $\gamma\gamma$, for which we obtain $\Gamma(\sigma \rightarrow \gamma\gamma) = (1.68 \pm 0.15)$ KeV.

1 Introduction

The study of the reaction $\gamma\gamma \rightarrow \pi^0\pi^0$ offers the possibility of having two neutral pions in the final state as a two body hadronic system. In this way, the interactions among pions can be unraveled more cleanly than in other processes where three or more hadrons appear in the final state. In this respect, the K_{e4}^{00} decays also share this property but limited to energies below the kaon mass. Furthermore, the two photon fusion also offers the interesting property of coupling mostly to the charged components of the hadronic states, while strong interactions are blind to that. Therefore, the study of $\gamma\gamma$ fusion into two hadrons displays new information on the inner constituents, beyond that obtained in direct strong scattering data. In addition, $\gamma\gamma \rightarrow \pi^0\pi^0$ has no either Born term, shown in fig.1 for charged mesons, so that final state interactions dominate this reaction. In this respect, one can think of the interest of precise data on this reaction to distinguish between present low energy parameterizations of the $\pi\pi$ isospin (I) 0 S-wave, to further study the nature of the σ resonance as well as that of the $f_0(980)$, and having another way to constraint their pole positions. The presence of the σ and its tight relation to chiral symmetry was clearly established from those non-perturbative methods [1–5] that resum unitarity in the series of Chiral Perturbation Theory (χ PT) [6, 7]. These methods were the first to show that the presence of a σ pole is not incompatible with the non-linear σ models. They also showed a clear convergence in the σ pole position when using either lowest order or one or two loop χ PT in the resummation, this is discussed in detail in ref.[5]. Recently, its associated pole was determined by solving Roy equations together with constraints from χ PT to two loops [8]. Other recent determinations are refs.[9, 10].

The reaction $\gamma\gamma \rightarrow \pi^0\pi^0$ is also an interesting ground test for χ PT [6, 7], since at lowest order is zero and at next-to-leading order (one loop) it is a prediction free of any counterterm [11, 12]. The one loop χ PT calculations were performed before the advent of data but the prediction just above threshold departs rapidly from experiment [13] and only the order of magnitude was rightly foreseen. A two loop χ PT calculation was done in refs.[14, 15], where the agreement with data [13] at low energies was improved. The three counterterms that appeared at $\mathcal{O}(p^6)$ were fixed by the resonance saturation hypothesis [16]. Other approaches supplying higher orders to one loop χ PT by taking into account unitarity [17] plus also crossed exchange resonances [18, 19] followed. Ref.[19] is a dynamical approach, with higher predictive power than dispersion relations (which make use of extensive experimental input from other related processes), though more model dependent. Ref.[19] is a Unitary χ PT (U χ PT) calculation in production processes [19–24] and was able to simultaneously describe $\gamma\gamma \rightarrow \pi^0\pi^0$, $\pi^+\pi^-$, $\eta\pi^0$, K^+K^- and $K^0\bar{K}^0$ from threshold up to rather high energies, $s^{1/2} \lesssim 1.5$ GeV. This approach was also used in ref.[25] to study the $\eta \rightarrow \pi^0\gamma\gamma$ decay.

Recently, ref.[26], making use of the approach of refs.[27, 28], focused on the low energy part of the reaction $\gamma\gamma \rightarrow \pi^0\pi^0$. Ref.[26] emphasizes the calculation of the $\gamma\gamma$ coupling of the σ as a way to deepen in the understanding of its nature. This approach was extended in ref.[29] so as to largely remove the sensitivity for lower energies, $\sqrt{s} \lesssim 0.8$ GeV, on the uncertainty in the not precisely known phase of the $I = 0$ S-wave $\gamma\gamma \rightarrow \pi\pi$ amplitude above the $K\bar{K}$ threshold. The novelty was to include a further subtraction in the dispersion relation for the $I = 0$ S-wave $\gamma\gamma \rightarrow \pi\pi$, together with an extra constraint to fix the additional subtraction constant. This was motivated by the use of an improved $I = 0$ S-wave Omnès function in the lines of ref.[30]. We

shall here extend the findings of ref.[29] and discuss in detail how the $f_0(980)$ peak, clearly seen recently in $\gamma\gamma \rightarrow \pi^+\pi^-$ [31], can be generated within the dispersive method of ref.[29]. We also show how this can be used to fix rather accurately the phase of the $I = 0$ S-wave $\gamma\gamma \rightarrow \pi\pi$ amplitude above the $K\bar{K}$ threshold. As a result, the remaining ambiguity in this phase by π in ref.[29] is removed. Interestingly, this allows to sharpen the prediction of the $\gamma\gamma \rightarrow \pi^0\pi^0$ cross section for $\sqrt{s} \lesssim 0.8$ GeV, up to the onset of D-waves, as compared with ref.[29]. This could then be used to constraint further different parameterizations of the low energy $\pi\pi$ $I = 0$ S-wave. We also offer explicit expressions for several axial-vector and vector crossed exchange contributions to $\gamma\gamma \rightarrow \pi\pi$, that are used in the present analysis and that of ref.[29]. The Unitary χ PT (U χ PT) calculation of ref.[19] on $\gamma\gamma \rightarrow \pi\pi$ will be reviewed and extended, so as to incorporate the same vector and axial-vector exchange contributions as in the dispersive analysis. We finally discuss the σ coupling to $\gamma\gamma$ and determine $\Gamma(\sigma \rightarrow \gamma\gamma) = (1.68 \pm 0.15)$ KeV. Other papers devoted to the calculation of the two photon decay widths of hadronic resonances are [32–43].

The content of the paper is as follows. In section 2 we discuss the dispersive method of ref.[27] and its extension by ref.[29] for calculating $\gamma\gamma \rightarrow \pi\pi$. Here we pay attention to the intrinsic difficulties of the approach of refs.[26–28] to generate the $f_0(980)$ peak in $\gamma\gamma \rightarrow \pi\pi$ and how this is overcome by the approach of ref.[29]. In this way, one can use this extra information to improve the calculation at lower energies. In section 3 we discuss and revise the U χ PT approach of ref.[19]. We also give in this section several formulae corresponding to the Born terms and exchanges of vector and axial-vector resonances to be used as input in both approaches. The resulting cross section $\sigma(\gamma\gamma \rightarrow \pi^0\pi^0)$ is discussed in section 4. The $\gamma\gamma$ decay width of the σ resonance and its coupling to $\gamma\gamma$ is considered in section 4.3. Conclusions are elaborated in section 5.

2 Dispersive approach to $\gamma\gamma \rightarrow \pi\pi$

We first review the approach of refs.[26–28] to establish a dispersion relation to calculate the two photon amplitude to $\pi\pi$. This approach has a large uncertainty above $\sqrt{s} \gtrsim 0.5$ GeV, which dramatically rises with energy such that for $\sqrt{s} = 0.5, 0.55, 0.6$ and 0.65 GeV it is 20, 45, 92 and 200 %, see fig.3 of ref.[26]. This uncertainty was largely reduced by the extended method of ref.[29]. We discuss here how this method allows to disentangle also the role of the $f_0(980)$ resonance in $\gamma\gamma \rightarrow \pi\pi$ and the way that this can be used to sharpen further the results of ref.[29].

2.1 Dispersion relation and Omnès function

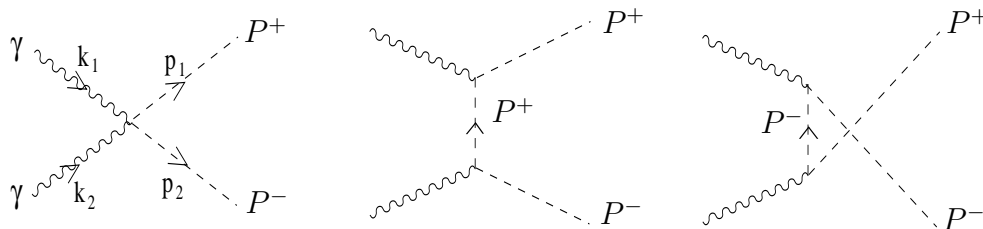


Figure 1: Born term contribution to $\gamma(k_1)\gamma(k_2) \rightarrow P^+(p_1)P^-(p_2)$.

Due to the null charge of the π^0 there is no Born term, shown in fig.1, for $\gamma\gamma \rightarrow \pi^0\pi^0$. As remarked in ref.[28], one then expects that only the S-wave would be the important partial wave at low energies, $\sqrt{s} \lesssim 0.6 - 0.7$ GeV. For $\gamma\gamma \rightarrow \pi^+\pi^-$, where there is a Born term because of the exchange of charged pions, the D-waves have a relevant contribution already at surprisingly low energies due to the smallness of the pion mass. In the following, we shall restrict ourselves to the S-wave contribution to $\gamma\gamma \rightarrow \pi\pi$, being particularly interested in the low energy region. Explicit calculations [19] show that the D-wave contribution in the $\gamma\gamma \rightarrow \pi^0\pi^0$ cross section at $\sqrt{s} \simeq 0.65$ GeV amounts less than a 10%, and this rapidly decreases for lower energies. Let us consider the S-wave amplitude $\gamma\gamma \rightarrow (\pi\pi)_I$, $F_I(s)$, where the two pions have definite $I = 0$ or 2. Notice that charge conjugation of the photons is even and this, together with Bose symmetry, excludes odd orbital angular momentum (and hence odd isospins) for the two pions. The function $F_I(s)$ on the complex s -plane is analytic except for two cuts, the unitarity one for $s \geq 4m_\pi^2$ and the left hand cut for $s \leq 0$, with m_π the pion mass. Let us denote by $L_I(s)$ the complete left hand cut contribution of $F_I(s)$. Then the function $F_I(s) - L_I(s)$, by construction, has only right hand cut.

Refs.[26–28] consider the Omnès function $\omega_I(s)$,

$$\omega_I(s) = \exp \left[\frac{s}{\pi} \int_{4m_\pi^2}^{\infty} \frac{\phi_I(s')}{s'(s' - s)} ds' \right], \quad (2.1)$$

with $\phi_I(s)$ the phase of $F_I(s)$ modulo π , chosen in such a way that $\phi_I(s)$ is *continuous* and $\phi_I(4m_\pi^2) = 0$. This function was criticized in ref.[30]. The $I = 0$ S-wave phase shift, $\delta_\pi(s)_0$, has a rapid increase by π around $s_K = 4m_K^2$, with m_K the kaon mass, due to the narrowness of the $f_0(980)$ resonance on top of the $K\bar{K}$ threshold. Let us denote by $\varphi(s)$ the phase of the $\pi\pi \rightarrow \pi\pi$ $I = 0$ S-wave strong amplitude such that it is continuous, modulo π when crossing a zero, and $\varphi(4m_\pi^2) = 0$. This phase is shown in fig.2 together with $\delta_\pi(s)_0$ and $\delta_\pi(s)_2$, where the latter is the $\pi\pi$ $I = 2$ phase shift. Now, if one uses $\varphi(s)$ instead of $\phi_0(s)$ in eq.(2.1) for illustration, the function $\omega_0(s)$ is discontinuous in the transition from $\delta_\pi(s_K)_0 \rightarrow \pi - \epsilon$ to $\delta_\pi(s_K)_0 \rightarrow \pi + \epsilon$, $\epsilon \rightarrow 0^+$. In the former case $|\omega_0(s)|$ has a zero, while in the latter it becomes $+\infty$. This discontinuity is illustrated in fig.3 by considering the difference between the dashed and dot-dashed lines, respectively. This discontinuous behaviour of $\omega_0(s)$ under small (even tiny) changes of $\delta_\pi(s)_0$ around s_K was the reason for the controversy regarding the value of the pion scalar radius $\langle r^2 \rangle_s^\pi$ between refs.[44–46] and ref.[47]. This controversy was finally solved in ref.[30] where it is shown that Ynduráin's method is compatible with the solutions obtained by solving the Muskhelishvili-Omnès equations for the scalar form factor [48–50]. The problem arose because refs.[44, 45] overlooked the proper solution and stuck to an unstable one.

Given the definition of the phase function $\phi_I(s)$ in eq.(2.1) the function $F_I(s)/\omega_I(s)$ has no right hand cut. Then, refs.[26–28] perform a twice subtracted dispersion relation of $(F_I(s) - L_I(s))/\omega_I(s)$,

$$F_I(s) = L_I(s) + a_I \omega_I(s) + c_I s \omega_I(s) + \frac{s^2}{\pi} \omega_I(s) \int_{4m_\pi^2}^{\infty} \frac{L_I(s') \sin \phi_I(s')}{s'^2 (s' - s) |\omega_I(s')|} ds'. \quad (2.2)$$

Low's theorem [51] implies that $F_I \rightarrow B_I(s)$ for $s \rightarrow 0$, with B_I the Born term contribution, shown in fig.1. If we write $L_I = B_I + R_I$, with $R_I \rightarrow 0$ for $s \rightarrow 0$, as can always be done, then the Low's theorem implies also that $F_I - L_I \rightarrow 0$ for $s \rightarrow 0$ and hence $a_I = 0$.

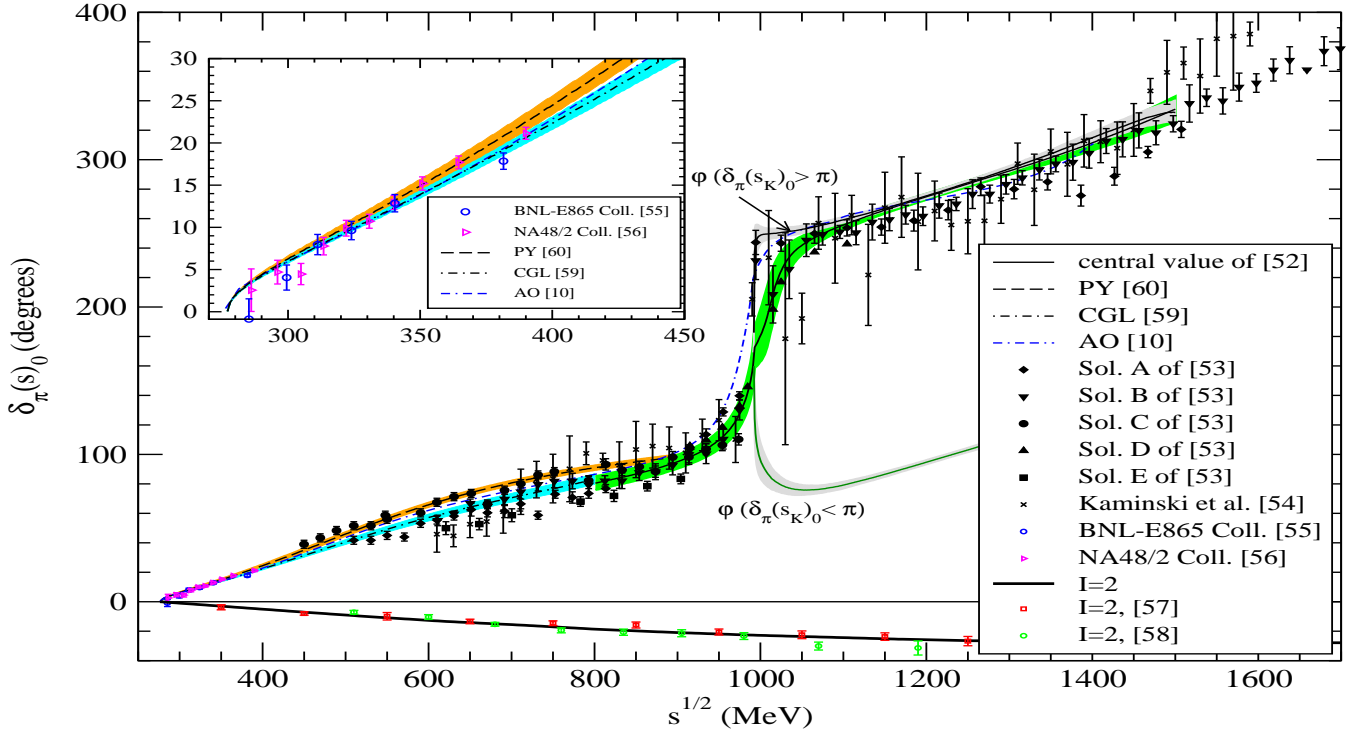


Figure 2: The phase shifts $\delta_\pi(s)_0$ and $\delta_\pi(s)_2$ and the phase $\varphi(s)$. Experimental data are from refs.[52–56] for $I = 0$ and refs.[57, 58] for $I = 2$. The insert is the comparison of CGL [59], dot-dashed line, PY [60], dashed line, and AO [10], double-dash-dotted line, with the accurate data from K_{e4} [55, 56]. For AO we have not shown its error bar in order not to overload the figure, see fig.1 of ref.[10] where it is given.

For the exotic $I = 2$ S-wave one can invoke Watson’s final state theorem^{#1} so that $\phi_2(s) = \delta_\pi(s)_2$. For $I = 0$ the same theorem guarantees that $\phi_0(s) = \delta_\pi(s)_0$ for $s \leq 4m_K^2$. Here one neglects the inelasticity due to the 4π and 6π states below the two kaon threshold, an accurate assumption as indicated by experiment [52, 53]. Above the two kaon threshold $s_K = 4m_K^2$, the phase function $\phi_0(s)$ cannot be fixed *a priori* due the onset of inelasticity. This is why ref.[26] took for $s > s_K$ that either $\phi_0(s) \simeq \delta_\pi(s)_0$ or $\phi_0(s) \simeq \delta_\pi(s)_0 - \pi$, in order to study the size of the uncertainty induced for lower energies. It results, as mentioned above, that this uncertainty becomes huge already for $\gtrsim 0.55$ GeV [26].

Let us now explain how this problem was settled in ref.[29]. Inelasticity is again small for $1.1 \lesssim \sqrt{s} \lesssim 1.5$ GeV [52, 53]. As remarked in refs.[30, 44], one can then apply approximately Watson’s final state theorem and for $F_0(s)$ this implies that $\phi_0(s) \simeq \delta^{(+)}(s)$ modulo π . Here $\delta^{(+)}(s)$ is the eigenphase of the $\pi\pi$, $K\bar{K}$ $I = 0$ S-wave S-matrix such that it is continuous and $\delta^{(+)}(s_K) = \delta_\pi(s_K)_0$. In refs.[30, 45] it is shown that $\delta^{(+)}(s) \simeq \delta_\pi(s)_0$ or $\delta_\pi(s)_0 - \pi$, depending on whether $\delta_\pi(s_K)_0 \geq \pi$ or $< \pi$, respectively. In order to fix the integer factor in front of π in the relation $\phi_0(s) \simeq \delta^{(+)}(s)$ modulo π , one needs to devise an argument to follow the possible trajectories of $\phi_0(s)$ in the *narrow* region $1 \lesssim \sqrt{s} \lesssim 1.1$ GeV, where inelasticity is not negligible.

^{#1}This theorem implies that the phase of $F_I(s)$ when there is no inelasticity is the same, modulo π , as the one of the isospin I S-wave $\pi\pi$ elastic strong amplitude.

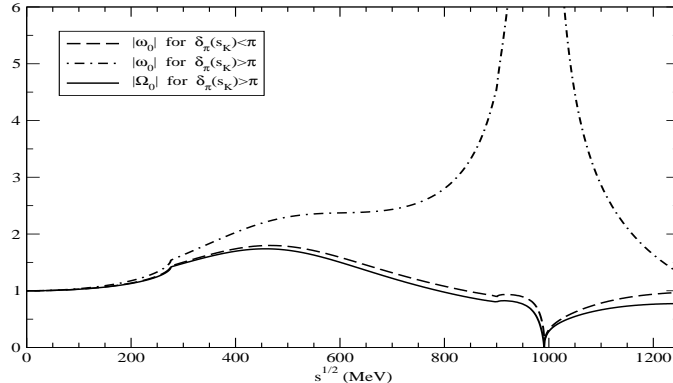


Figure 3: $|\omega_0(s)|$ from eq.(2.1) with $\delta_\pi(s_K)_0 < \pi$, dashed-line, and $\delta_\pi(s_K)_0 > \pi$, dot-dashed line. The solid line corresponds to the use of $\Omega_0(s)$ in eq.(2.3) for the latter case. Here $\varphi(s)$ is used as $\phi_0(s)$ in eq.(2.1) for illustrative purposes.

The remarkable physical effects happening there are the appearance of the $f_0(980)$ resonance on top of the $K\bar{K}$ threshold and the cusp effect of the latter that induces a discontinuity at s_K in the derivative of observables, this is clearly visible in fig.2. Between 1.05 to 1.1 GeV there are no further narrow structures and observables evolve smoothly. Approximately half of the region between 0.95 and 1.05 GeV is elastic and $\phi_0(s) = \delta_\pi(s)_0$ (Watson's theorem), so that it rises rapidly. Above $2m_K \simeq 1$ GeV and up to 1.05 GeV the function $\phi_0(s)$ can keep increasing with energy, like $\delta_\pi(s)_0$ or $\varphi(s)$ for $\delta_\pi(s_K)_0 \geq \pi$, and this is always the case for the corresponding phase function of the strange scalar form factor of the pion [30]. It is also the behaviour for $\phi_0(s)$ corresponding to the explicit calculation of ref.[19]. The other possibility is a change of sign in the slope at s_K due to the $K\bar{K}$ cusp effect such that $\phi_0(s)$ starts a rapid decrease in energy, like $\varphi(s)$ for $\delta_\pi(s_K)_0 < \pi$, fig.2. Above $\sqrt{s} = 1.05$ GeV, $\phi_0(s)$ matches smoothly with the behaviour for $\sqrt{s} \gtrsim 1.1$ GeV, which it is worth recalling that it is constraint by Watson's final state theorem. As a result of this matching, for $\sqrt{s} \gtrsim 1$ GeV *either* $\phi_0(s) \simeq \delta_\pi(s)_0$ *or* $\phi_0(s) \simeq \delta_\pi(s) - \pi$, corresponding to an increasing or decreasing $\phi_0(s)$ above s_K , in order. Our argument also justifies the similar choice of phases in ref.[26] above s_K to estimate uncertainties.

Let us define the switch z to characterize the behaviour of $\phi_0(s)$ for $s > s_K$, and close to s_K , such that $z = +1$ if $\phi_0(s)$ rises with energy and $z = -1$ if it decreases. Let s_1 be the value of s at which $\phi_0(s_1) = \pi$. As shown in ref.[30], instead of eq.(2.1), one should better consider the Omnès function,

$$\Omega_0(s) = \left(1 - \theta(z) \frac{s}{s_1}\right) \exp \left[\frac{s}{\pi} \int_{4m_\pi^2}^{\infty} \frac{\phi_0(s')}{s'(s' - s)} ds' \right], \quad (2.3)$$

with $\theta(z) = 1$ for $z = +1$ and 0 for $z = -1$. Because of the first order polynomial in $\Omega_0(s)$, with a zero at s_1 , one can guarantee a continuous behaviour for $\Omega_0(s)$ when moving from $z = -1$ to $z = +1$, passing from a deep minimum to a zero. This is shown in fig.3 by comparing the solid line with the dashed one, both computed with eq.(2.3) and using $\varphi(s)$ as $\phi_0(s)$ for illustrative purposes. Both lines are very close to each other as corresponds to a continuous transition. Note that s_1 is the only point around s_K where the imaginary part of $\omega_0(s)$ vanishes, and this fixes unambiguously the position of the zero in eq.(2.3), as discussed in ref.[30]. For $I = 2$ since the

phase shifts are small and smooth [57, 58], see fig.2, the issue of the discontinuity under changes in the parameterizations does not arise and we keep using $\omega_2(s)$, eq.(2.1).

Now, we perform a twice subtracted dispersion relation for $(F_0(s) - L_0(s))/\Omega_0(s)$, employing $\Omega_0(s)$ instead of $\omega_0(s)$. Instead of eq.(2.2) one obtains

$$F_0(s) = L_0(s) + c_0 s \Omega_0(s) + \frac{s^2}{\pi} \Omega_0(s) \int_{4m_\pi^2}^{\infty} \frac{L_0(s') \sin \bar{\phi}_0(s')}{s'^2 (s' - s) |\Omega_0(s')|} ds' + \theta(z) \frac{\omega_0(s)}{\omega_0(s_1)} \frac{s^2}{s_1^2} (F_0(s_1) - L_0(s_1)) . \quad (2.4)$$

In the previous equation we introduce $\bar{\phi}_0(s)$ that is defined as the phase of $\Omega_0(s)$. Let us note that in the case $z = +1$ the phase of $\Omega_0(s)$ for $s > s_1$ is not $\phi_0(s)$ but $\phi_0(s) - \pi$, due to the factor $1 - (s + i\epsilon)/s_1$ in $\Omega_0(s)$, eq.(2.3), present in this case. For $I = 2$ we use eq.(2.2).

It is worth mentioning that eq.(2.4) for $I = 0$ and $z = +1$ is equivalent to perform a three times subtracted dispersion relation for $(F_0(s) - L_0(s))/\omega_0(s)$, instead of the twice subtracted dispersion relation in eq.(2.2) as proposed in refs.[26–28]. In eq.(2.4), two subtractions are taken at $s = 0$ and a third one at s_1 . We could have taken the third subtraction at $s = 0$ as well, so that for $z = +1$ one has

$$F_0(s) = L_0(s) + c_0 s \omega_0(s) + d_0 s^2 \omega_0(s) + \frac{s^3 \omega_0(s)}{\pi} \int_{4m_\pi^2}^{\infty} \frac{L_0(s') \sin \phi_0(s')}{s'^3 (s' - s) |\omega_0(s')|} ds' , \quad (2.5)$$

Nevertheless, we find more convenient eq.(2.4) as it is physically motivated by the use of the Omnès function eq.(2.3) that is continuous under changes in the parameterization of the $I = 0$ S-wave S-matrix. Furthermore, eq.(2.4) is more suited to constraint the $f_0(980)$ energy region in order to implement the condition **3** below, because $s_1 \simeq 1 \text{ GeV}^2$ and it coincides very approximately with the mass of this resonance.

Let us denote by $F_N(s)$ the S-wave $\gamma\gamma \rightarrow \pi^0\pi^0$ amplitude and by $F_C(s)$ the $\gamma\gamma \rightarrow \pi^+\pi^-$ one. The relation between F_0 , F_2 and $F_N(s)$, $F_C(s)$ is

$$\begin{aligned} F_N(s) &= -\frac{1}{\sqrt{3}} F_0 + \sqrt{\frac{2}{3}} F_2 , \\ F_C(s) &= -\frac{1}{\sqrt{3}} F_0 - \sqrt{\frac{1}{6}} F_2 . \end{aligned} \quad (2.6)$$

We are still left with the unknown constants c_0 , c_2 for $I = 0$ and 2, respectively, and $F_0(s_1) - L_0(s_1)$ for $I = 0$ and $z = +1$. In order to determine them we impose the following conditions:

1. $F_C(s) - B_C(s)$ vanishes linearly in s for $s \rightarrow 0$ and we match the coefficient to the one loop χ PT result [11, 12].
2. $F_N(s)$ vanishes linearly for $s \rightarrow 0$ as well and the coefficient can be obtained again from one loop χ PT [11, 12].
3. For $I = 0$ and $z = +1$ one has in addition the constant $F_0(s_1) - L_0(s_1)$. Its value can be restricted taking into account that $F_N(s)$ has an Adler zero, due to chiral symmetry. This zero is located at $s_A = m_\pi^2$ in one loop χ PT and moves to $s_A = 1.175 m_\pi^2$ in two loop χ PT [14]. A rather large correction around 18% results, which prevents us from taking s_A straightforwardly as given by χ PT. In turn, we obtain that the value of the resulting cross section $\sigma(\gamma\gamma \rightarrow \pi^0\pi^0)$ around the

$f_0(980)$ resonance is quite sensitive to the value of $F_0(s_1) - L_0(s_1)$. This is so because this constant appears in the last term in eq.(2.4) which dominates the energy region around the $f_0(980)$ since $\Omega_0(s_1) = 0$. Though the dispersive method is devised at its best for lower energies, it is also clear that it should give, at least, the proper order of magnitude for $\sigma(\gamma\gamma \rightarrow \pi^0\pi^0)$ in the $f_0(980)$ region. E.g., other models [19, 61, 62] having similar basic ingredients describe that energy region quite well indeed. We then restrict $F_0(s_1) - L_0(s_1)$ so that $\sigma(\gamma\gamma \rightarrow \pi^0\pi^0) \leq 40$ nb at s_1 . Note that the D-wave component of this cross-section at $s_1 \simeq 1$ GeV, due to the tail of the $f_2(1270)$ resonance, is not longer small and hence the S-wave contribution should be significantly smaller than the experimental value < 40 nb. This is clearly shown by experiment [13], see fig.9. The S- and D-wave contributions add incoherently in the total cross section because of the integration on the azimuthal angle as the $f_2(1270)$ resonance signal is overwhelming helicity 2 [27]. We have checked that this upper bound for the peak of the $f_0(980)$ in $\gamma\gamma \rightarrow \pi^0\pi^0$ is equivalent to impose that the $\gamma\gamma$ width of the $f_0(980)$, $\Gamma(f_0(980) \rightarrow \gamma\gamma)$, lies in the range $205_{-83}^{+95}(\text{stat})_{-117}^{+147}(\text{sys})$ eV, determined by the Belle Collaboration in ref.[31]. The width $\Gamma(f_0(980) \rightarrow \gamma\gamma)$ is calculated analogously as done in section 4.3 for the $\gamma\gamma$ width of the σ resonance. We shall see that the effect of this rather large uncertainty allowed at 1 GeV, see fig.9, is very mild at lower energies, as shown in fig.6.

It is worth discussing further the improvement achieved by eq.(2.4), first derived in ref.[29], in the understanding of the role played by the $f_0(980)$ resonance in $\gamma\gamma \rightarrow \pi\pi$. The resulting $|F_0(s)|$ given by eq.(2.2) from ref.[26] explodes for $z = +1$ around s_1 , as $|w_0(s)|$ becomes extremely large for this energy as shown in fig.3 by the dot-dashed line. To avoid this large number the coefficient of $w_0(s_1)$ in eq.(2.2) is required to almost vanish,

$$c_0 + \frac{s_1}{\pi} \int_{4m_\pi^2}^{\infty} \frac{L_0(s') \sin \phi_0(s')}{s'^2 (s' - s_1) |\omega_0(s')|} \simeq 0 . \quad (2.7)$$

Thus, a dramatic fine tuning of $\phi_0(s)$ is implied, so as the integral above must almost cancel c_0 . Note that c_0 is a real number and this integral is real only at $s = s_1$, precisely where it is evaluated. Then the cancellation in eq.(2.7) is possible. But c_0 , following the approach of ref.[26, 28], is already determined by the requirement that the Adler zero for $F_N(s)$ is at $s_A = m_\pi^2/2$, m_π^2 or $2m_\pi^2$ [26]. The subsequent uncertainty in c_0 , together with the uncertainty in the knowledge of $\phi_0(s)$ above the $K\bar{K}$ threshold, invalidates in practice the fine tuning in eq.(2.7). This makes that the results of ref.[26] for $\sigma(\gamma\gamma \rightarrow \pi^0\pi^0)$ diverge rapidly with energy above $\sqrt{s} \simeq 0.5$ GeV for $z = +1$ as remarked above, see fig.3 of ref.[26]. Refs.[18, 27, 28] did not discuss this source of large uncertainty in their calculations but, since these papers follow the same scheme as ref.[26], it is certainly present. One of the main results that follow from eq.(2.4) is to showing that by using $\Omega_0(s)$ one can cure such diverging results for $z = +1$. This issue is solved because for s around s_1 one has that $\Omega_0(s) \simeq 0$ and the diverging effects due to $\omega_0(s)$ for $z = +1$ are isolated in the last term and controlled by the factor $F_0(s_1) - L_0(s_1)$. The small signal of the $f_0(980)$ implicit in the $\sigma(\gamma\gamma \rightarrow \pi^0\pi^0)$ data of ref.[13], and explicitly seen in $\gamma\gamma \rightarrow \pi^+\pi^-$ [31], implies a vanishing value of the constant $F_0(s_1) - L_0(s_1)$. In our actual calculations we obtain typically $(F_0(s_1) - L_0(s_1))/L_0(s_1) \lesssim 10^{-2}$. One can indeed understand the smallness of this number by a continuity argument. For that, let us envisage a mathematical continuous transition from $z = -1$ to $z = +1$ by taking $\varphi(s)$ as $\phi_0(s)$ in eq.(2.4). The situation $z = -1$ is accomplished when $\delta_\pi(s_K)_0 < \pi$ and $z = +1$ when $\delta_\pi(s_K)_0 \geq \pi$, see fig.2. Now, imposing that $F_0(s)$ is continuous under the transition $\delta_\pi(s_K)_0 \rightarrow \pi - \epsilon$ (where the

last term in eq.(2.4) is absent) to $\delta_\pi(s_K)_0 \rightarrow \pi + \epsilon$, $\epsilon \rightarrow 0^+$, where it is present, implies that $F_0(s_1) - L_0(s_1) = 0$ for $\delta_\pi(s_K)_0 = 0$. Since $\phi_0(s)$ is quite close to $\varphi(s)$ both for $z = +1$ and -1 , the continuous transition considered is not just academic because $\delta_\pi(s_K) \simeq \pi$.^{#2} As a result one should expect that $F_0(s_1) - L_0(s_1) \simeq 0$.

Since the $f_0(980)$ resonance gives rise to a small *peak* in the precise data on $\gamma\gamma \rightarrow \pi^+\pi^-$ [31], then $\phi_0(s)$ must increase with energy above s_K and the case with $z = +1$ is the one realized in nature. As a result $\phi_0(s) \simeq \delta_\pi(s)_0$, at least up to around $\sqrt{s} \lesssim 1.5$ GeV. Otherwise $z = -1$ in eq.(2.4) and because $|\omega_0(s)|$ has a deep around the $f_0(980)$ mass there is no a local maximum associated with this resonance in $|F_0(s)|$ but a minimum. One should keep in mind that $z = +1$ and only this case will be considered in the subsequent.

In ref.[29] both cases $z = \pm 1$ were discussed and kept, so that the differences in the results by taking one case or the other were included in the uncertainties of the approach, e.g. when presenting $\sigma(\gamma\gamma \rightarrow \pi^0\pi^0)$ for $\sqrt{s} \lesssim 0.8$ GeV. In the latter reference the main focus was driven towards the drastic reduction of the uncertainty in the results for the two choices of $\phi_0(s)$ above s_K . Here we are more accurate as we have singled out the $z = +1$ case as the proper one for $\phi_0(s)$ and $s > s_K$.

We can estimate the uncertainty in the approximate relation $\phi_0(s) \simeq \delta_\pi(s)_0$ for $4m_K^2 \lesssim \sqrt{s} \lesssim 1.5$ GeV by similar arguments to those employed in ref.[30]. Let the $\pi\pi$ and $K\bar{K}$ $I = 0$ S-wave S-matrix,

$$S = \begin{pmatrix} \eta e^{2i\delta_\pi} & i\sqrt{1-\eta^2}e^{i(\delta_\pi+\delta_K)} \\ i\sqrt{1-\eta^2}e^{i(\delta_\pi+\delta_K)} & \eta e^{2i\delta_K} \end{pmatrix}, \quad (2.8)$$

with η the elasticity parameter. This matrix is diagonalized with the orthogonal matrix C ,

$$C = \begin{pmatrix} \cos \theta & \sin \theta \\ -\sin \theta & \cos \theta \end{pmatrix}. \quad (2.9)$$

In eq.(2.8) $\delta_\pi \equiv \delta_\pi(s)_0$ and δ_K is the kaon phase shifts. Explicit expressions for $\cos \theta$ and $\sin \theta$ in terms of the $I = 0$ S-wave $\pi\pi$ and $K\bar{K}$ phase shifts and the elasticity parameter are given in ref.[30]. In this reference one can also find the expression for the eigenvalues $e^{2i\delta^{(+)}}$ and $e^{2i\delta^{(-)}}$. This diagonalization allows to disentangle two elastic scattering channels and then the two photon $I = 0$ S-wave amplitudes attached to every of these channels, Γ'_1 and Γ'_2 , will satisfy the Watson's final state theorem in the whole energy range. Because of this diagonalization one has,

$$\begin{aligned} F &\equiv \begin{pmatrix} F_0 \\ F_K \end{pmatrix} = CF' = C \begin{pmatrix} \Gamma'_1 \\ \Gamma'_2 \end{pmatrix}, \\ F_0 &= \cos \theta \Gamma'_1 + \sin \theta \Gamma'_2, \\ F_K &= \cos \theta \Gamma'_2 - \sin \theta \Gamma'_1. \end{aligned} \quad (2.10)$$

Here F_K is the $I = 0$ S-wave $\gamma\gamma \rightarrow K\bar{K}$ amplitude. Now, when $\eta \rightarrow 1$ then $\sin \theta \rightarrow 0$ as $\epsilon = \sqrt{(1-\eta)/2}$ [30] and $F_0(s)$ is given approximately by $\Gamma'_1(s)$. With $\tan \theta \Gamma'_2/\Gamma'_1 = \epsilon e^{i\rho}$, we

^{#2}See ref.[45] for a detailed discussion on the value of $\delta_\pi(s_K)$.

rewrite F_0 above as,

$$\begin{aligned}
F_0(s) &= \cos \theta \Gamma'_1 [1 + \epsilon(\cos \rho + i \sin \rho)] \\
&= \cos \theta \Gamma'_1 (1 + \epsilon \cos \rho) \left(1 + \frac{i\epsilon \sin \rho}{1 + \epsilon \cos \rho} \right) \\
&= \cos \theta \Gamma'_1 (1 + \epsilon \cos \rho) e^{i\lambda} + \mathcal{O}(\epsilon^2) .
\end{aligned} \tag{2.11}$$

with $\lambda = \epsilon \sin \rho / (1 + \epsilon \cos \rho)$. From the previous equation it follows that

$$\phi_0(s) = \delta_\pi(s)_0 + \lambda + \mathcal{O}(\epsilon^2) \tag{2.12}$$

with $\epsilon \rightarrow 0$ for $\eta \rightarrow 1$. Using $\eta = 0.8$ in eq.(2.12) for the range $1.1 \lesssim \sqrt{s} \lesssim 1.5$ GeV (from the K-matrix in eq.(4.44) $\eta \simeq 1$), one ends with $|\epsilon| \simeq 0.3$. Taking into account that $\delta_\pi(s)_0$ is larger than $3\pi/2$, fig.2, then one has a relative correction of around a 10%. We can also proceed similarly in the region $1 \lesssim \sqrt{s} \lesssim 1.1$ GeV. Applying now eq.(2.12) with $\eta \gtrsim 0.6$ from the $\pi\pi \rightarrow K\bar{K}$ scattering experiments [63], and taking $\delta_\pi(s)_0 \geq \pi$ in the previous energy range, we end up with a $\sim 20\%$ uncertainty. We shall incorporate in our error analysis the previous uncertainties.

We now consider the phases used above $s_H \equiv 2.25$ GeV². For $I = 2$, where final state interaction give rise to small corrections, we directly take the extrapolation of our fits. Notice that due to the way that the vector and axial-vector exchanges are calculated from the chiral Lagrangians presented in the next section, one has that $L_I(s)$ diverges linearly in s for $s \rightarrow +\infty$. On the other hand $|\omega_I(s)| \propto s^{-\nu_I}$ with $\nu_I = \phi_I(\infty)/\pi$. Taking this into account for $I = 2$ the integrand in eq.(2.2) tends to $\sin \phi_2(s') s'^{\nu_2-1} / (s' - s)$ for $s' \rightarrow +\infty$, with $|\nu_2| \ll 1$, and then the dispersion integral converges. For $I = 0$ we have that $|\Omega_0(s)|$ behaves as $s^{-\nu_0+1}/s_1$ for $s \rightarrow +\infty$. We know already $\phi_0(s)$ for s quite high, and noticing that $\phi_0(s_H)/\pi \simeq 2$ we take this value as a good approximation for ν_0 so that $\Omega_0(s) \propto s^{-1}$ and $\phi_0(+\infty) = 2\pi$. The integrand in eq.(2.4) tends then to $\sin \phi_0(s') / (s' - s)$ and converges because $\sin \phi_0(\infty) \rightarrow 0$. As a soft extrapolation for $\phi_0(s)$ for $s > s_H$ we shall take the same expression as in ref.[30] with 2π as the limiting value,

$$\phi_0(s) = 2\pi \left(1 \pm \frac{1}{\log s/\Lambda^2} \right) , \quad s > s_H , \tag{2.13}$$

with $\Lambda^2 \in [0, 0.35]$ GeV². In this way at $s = s_H$ one has an uncertainty of $\sim \pm\pi/2$ degrees that narrows only logarithmically for higher energies. This uncertainty is incorporated in the error analyses that follow. We think that our choices for $\phi_I(s)$ for $s > s_H$, and the uncertainties taken, are quite reasonable. Let us note that for $s < 1$ GeV² the integrand in the dispersive integral is overwhelmingly dominated for $s' \ll s_H$.

3 Dynamical approach to $\gamma\gamma \rightarrow \pi\pi$.

In this section we review and update the approach of ref.[19] based on U χ PT. This approach extends the χ PT one loop calculation of $\gamma\gamma \rightarrow \pi^0\pi^0$, $\pi^+\pi^-$ and K^+K^- , implementing unitarity in coupled channels, in order to account of the meson-meson final state interactions, and by including vector and axial-vector resonance exchanges. For the derivation of the unitarization

formulae that we use below we refer to the original ref.[19], see also refs.[22, 23] for later advances in the formalism. In the dispersive method discussed in the previous section this is accomplished by the use of the Omnès functions $\Omega_0(s)$ and $\omega_2(s)$ in the dispersion relations eqs.(2.4) and (2.2), respectively.

On the other hand, we also offer here the expressions for the Born terms and the crossed exchanges of vector (1^{--}) and axial-vector (1^{++} , 1^{+-}) resonances, employed both in the dispersive and dynamical approaches. The exchange of vector resonances calculated from chiral Lagrangians was performed in ref.[64], while the inclusion of the 1^{++} axial ones was undertaken in ref.[65]. Here we have calculated these tree level graphs but our results are different to those of ref.[65] for the latter diagrams. Reassuringly, we agree with the expressions given in ref.[14] for the 1^{+-} axial-vector resonance exchanges, which are also included here, and that share the same Lorentz structure as the 1^{++} resonance exchange contributions. It is worth mentioning that the 1^{++} resonance exchanges contribute already at $\mathcal{O}(p^4)$ in χ PT for $\gamma\gamma \rightarrow \pi^+\pi^-$, while the other resonance exchanges start one order higher in $\gamma\gamma \rightarrow \pi\pi$. The formulae corresponding to the Born term and the different resonance exchanges are given below.

3.1 Formulae for F_N and F_C

The expressions for $F_N(s)$ and $F_C(s)$ of ref.[19] are enlarged now to include the exchanges of the K^* and the 1^{+-} axial-vector nonet:

$$\begin{aligned}
F_N &= T_{\omega,\pi^0\pi^0}^S + T_{C,\pi^0\pi^0}^S + T_{\rho,\pi^0\pi^0}^S + (\tilde{t}_{\rho\pi^0\pi^0} + \tilde{t}_{\omega\pi^0\pi^0} + \tilde{t}_{C\pi^0\pi^0}) t_{\pi^0\pi^0,\pi^0\pi^0} \\
&\quad + (\tilde{t}_{\chi\pi} + \tilde{t}_{\rho\pi^+\pi^-} + \tilde{t}_{A\pi^+\pi^-} + \tilde{t}_{C\pi^+\pi^-}) t_{\pi^+\pi^-, \pi^0\pi^0} \\
&\quad + (\tilde{t}_{\chi K} + 2\tilde{t}_{K^*K^+K^-} + \tilde{t}_{AK^+K^-} + 5\tilde{t}_{CK^+K^-}) t_{K^+K^-, \pi^0\pi^0} , \\
F_C &= T_B^S + T_{\rho,\pi^+\pi^-}^S + t_{A,\pi^+\pi^-}^S + t_{C,\pi^+\pi^-}^S + (\tilde{t}_{\rho\pi^0\pi^0} + \tilde{t}_{\omega\pi^0\pi^0} + \tilde{t}_{C\pi^0\pi^0}) t_{\pi^0\pi^0,\pi^+\pi^-} \\
&\quad + (\tilde{t}_{\chi\pi} + \tilde{t}_{\rho\pi^+\pi^-} + \tilde{t}_{A\pi^+\pi^-} + \tilde{t}_{C\pi^+\pi^-}) t_{\pi^+\pi^-, \pi^+\pi^-} \\
&\quad + (\tilde{t}_{\chi K} + 2\tilde{t}_{K^*K^+K^-} + \tilde{t}_{AK^+K^-} + 5\tilde{t}_{CK^+K^-}) t_{K^+K^-, \pi^+\pi^-} .
\end{aligned} \tag{3.14}$$

The different terms in this equation are given below. Although not explicitly indicated in the subscripts, the contributions from amplitudes with the intermediate $K^0\bar{K}^0$ state are encoded in the brackets proportional to $t_{K^+K^-, \pi\pi}$, because this S-wave strong amplitude is the same as $t_{K^0\bar{K}^0, \pi\pi}$ and kaon masses are all taken the same (isospin limit).

In the previous equations the strong S-wave amplitudes can be obtained from those with isospin defined as,

$$\begin{aligned}
t_{\pi^+\pi^-, \pi^+\pi^-} &= \frac{2}{3}t_{\pi\pi, \pi\pi}^{I=0} + \frac{1}{3}t_{\pi\pi, \pi\pi}^{I=2} , \\
t_{\pi^0\pi^0, \pi^0\pi^0} &= \frac{2}{3}t_{\pi\pi, \pi\pi}^{I=0} + \frac{4}{3}t_{\pi\pi, \pi\pi}^{I=2} , \\
t_{\pi^+\pi^-, \pi^0\pi^0} &= \frac{2}{3}t_{\pi\pi, \pi\pi}^{I=0} - \frac{2}{3}t_{\pi\pi, \pi\pi}^{I=2} , \\
t_{K^+K^-, \pi^0\pi^0} &= t_{K^+K^-, \pi^+\pi^-} = \frac{1}{\sqrt{3}}t_{K\bar{K}, \pi\pi}^{I=0} .
\end{aligned} \tag{3.15}$$

In ref.[19] the $I = 0$ and $I = 2$ S-wave amplitudes were calculated as in ref.[1]. For $I = 2$ we employ directly the experimental phase shifts $t_{\pi\pi,\pi\pi}^{I=2} = -\frac{8\pi\sqrt{s}}{q_\pi} e^{i\delta_\pi(s)^2} \sin \delta_\pi(s)_2$.

In eq.(3.14) the amplitudes $T_{\omega,\pi^0\pi^0}$, $T_{\rho,\pi\pi}$, $T_{K^*,K\bar{K}}$ are the crossed exchange of the ω , ρ and K^* vector resonances, in order, denoted generically by $T_{V,P\bar{P}}$. On the other hand, $T_{A,P\bar{P}}$ and $T_{C,P\bar{P}}$ refer to the exchange of the 1^{++} and 1^{+-} multiplets of axial-vector resonances, respectively. In addition, $\tilde{t}_{\chi P}$ represents the one loop χ PT function,

$$\tilde{t}_{\chi P}(s) = \frac{2e^2}{16\pi^2} \left\{ 1 + \frac{m_P^2}{s} \left[\log \frac{1 + \sigma_P(s)}{1 - \sigma_P(s)} - i\pi \right]^2 \right\}, \quad (3.16)$$

with m_P the mass of the pseudoscalar P , either π or K , and $\sigma_P(s) = \sqrt{1 - 4m_P^2/s}$. Finally, $\tilde{t}_{RP\bar{P}}$ corresponds to the unitarity loop with the pseudoscalars P , \bar{P} and the crossed exchange of the resonance R , either vector or axial, calculated as in ref.[19].

Here we give the expressions calculated for the Born terms, fig.1, $\gamma(k_1, \lambda_1)\gamma(k_2, \lambda_2) \rightarrow P^+(p_1)P^-(p_2)$,

$$T_B = 2e^2 \left[\epsilon_1\epsilon_2 - \frac{(\epsilon_1 p_1)(\epsilon_2 p_2)}{p_1 k_1 - i0^+} - \frac{(\epsilon_1 p_2)(\epsilon_2 p_1)}{p_1 k_2 - i0^+} \right], \quad (3.17)$$

where $\epsilon_1(k_1, \lambda_1)$, $\epsilon_2(k_2, \lambda_2)$ are the polarization vectors of the photons taken in the gauge $\epsilon_1 k_1 = \epsilon_1 k_2 = \epsilon_2 k_1 = \epsilon_2 k_2 = 0$, with polarizations given by λ_1 and λ_2 , respectively. In the following, we shall only need the three-momenta \vec{k}_1 and \vec{k}_2 along the z -axis and use the four-vectors $(0, \vec{\epsilon}(k, \lambda))$ with $\vec{\epsilon}(k\hat{z}, \pm) = \mp \frac{1}{\sqrt{2}}(\hat{x} \pm i\hat{y})$ and $\vec{\epsilon}(-k\hat{z}, \pm) = \mp \frac{1}{\sqrt{2}}(\hat{y} \pm i\hat{x})$. The projection of the Born term in S-wave is given by $i \int d\vec{p} T_B(\lambda_1 = +, \lambda_2 = +, \vec{p})/4\pi$, with \vec{p} the CM three-momentum of the pions. The prefactor i is included for convenience. An analogous formula for the projection in S-wave is employed for any other amplitude of $\gamma\gamma \rightarrow P\bar{P}$. We then have,

$$T_B^S = 2e^2 \frac{2m_\pi^2/s}{\sigma_\pi(s)} \log \frac{1 + \sigma_\pi(s)}{1 - \sigma_\pi(s)}, \quad (3.18)$$

with $\sigma_\pi = \sqrt{1 - 4m_\pi^2/s}$.

We now consider the crossed exchange of the vector resonances in $\gamma(k_1, \lambda_1)\gamma(k_2, \lambda_2) \rightarrow P(p_1)\bar{P}(p_2)$. We evaluate them employing the chiral Lagrangian [64],

$$\mathcal{L}_{VP\gamma} = R_\omega e \epsilon_{\mu\nu\alpha\beta} F^{\mu\nu} \text{Tr} [\Phi \{Q, \partial^\alpha V^\beta\}] , \quad (3.19)$$

where the matrix fields $\Phi(x)$, $V(x)$ contain the octet of pseudoscalars and vectors [64] and Q is the quark charge matrix, $Q = \text{diag}(2/3, -1/3, -1/3)$.

$$T_{V,P\bar{P}} = e^2 R_V^2 \left[\frac{(\epsilon_1\epsilon_2)[s(t + m_{\bar{P}}^2) - (t - m_\pi^2)(u - m_\pi^2)] - 2s(\epsilon_1 p_1)(\epsilon_2 p_1)}{t - M_V^2 + i0^+} + \frac{(\epsilon_1\epsilon_2)[s(u + m_P^2) - (t - m_\pi^2)(u - m_\pi^2)] - 2s(\epsilon_1 p_1)(\epsilon_2 p_1)}{u - M_V^2 + i0^+} \right] \quad (3.20)$$

with $P = \pi^0, \pi^\pm, K^\pm$ or K^0 and $V = \omega, \rho$ or K^* . Furthermore, $R_\rho^2 = R_{K^*}^2 = R_\omega^2/9$. In these expressions M_ω, M_ρ and M_{K^*} are the masses of the ω, ρ and K^* , respectively. The coupling R_ω^2

is determined from the width $\Gamma(\omega \rightarrow \gamma\pi^0)$,

$$R_\omega^2 = \frac{6}{\alpha} \frac{M_\omega^3}{(M_\omega^2 - m_\pi^2)^3} \Gamma(\omega \rightarrow \gamma\pi^0) = 1.44 \text{ GeV}^{-2}. \quad (3.21)$$

The projection of eq.(3.20) is given by,

$$T_{V, P\bar{P}}^S = -2e^2 R_V^2 \left[\frac{M_V^2}{\sigma_P} \log \frac{1 + \sigma_P + s_V/s}{1 - \sigma_P + s_V/s} - s \right], \quad (3.22)$$

with $s_V = 2(M_V - m_P^2)$. It is important to remark that eqs.(3.20) and (3.22) contribute at the level of a two loop χ PT calculation in $\gamma\gamma \rightarrow \pi\pi$. This implies that vector exchange is relatively suppressed at low energies due to its rather high chiral counting. Nonetheless in fig.4 it is shown that they are significant above 0.4 GeV. The 1^{++} axial-vector crossed exchanges, as we shall see immediately, appear already at the level of one loop χ PT. Hence, for low energy $\gamma\gamma \rightarrow \pi\pi$ their contributions are more important than those due to the exchange of vectors. To evaluate the contribution from the crossed exchanges of the 1^{++} axial resonances in $\gamma\gamma \rightarrow \pi^+\pi^-$ and $\gamma\gamma \rightarrow K^+K^-$ we consider the Lagrangian [16],

$$\mathcal{L}_{AP\gamma} = i \frac{eF_A}{2f_\pi} F^{\mu\nu} \text{Tr} (\Phi[Q, A_{\mu\nu}]) , \quad (3.23)$$

with $A_{\mu\nu}$ a matrix with the 1^{++} octet of axial resonances and f_π the pion decay constant. Here the antisymmetric tensor formalism for the axial-vector field is employed. The resulting amplitudes are

$$T_{A, \pi^+\pi^-} = e^2 \frac{F_A^2}{M_A^2 f_\pi^2} \left\{ s(\epsilon_1\epsilon_2) - \frac{1}{4} \frac{(\epsilon_1\epsilon_2)(t - m_\pi^2)^2 - 2s(\epsilon_1 p_1)(\epsilon_2 p_1)}{M_A^2 - t - i0^+} \right. \\ \left. - \frac{1}{4} \frac{(\epsilon_1\epsilon_2)(u - m_\pi^2)^2 - 2s(\epsilon_1 p_1)(\epsilon_2 p_1)}{M_A^2 - u - i0^+} \right\} , \quad (3.24)$$

and the same expression for T_{A, K^+K^-} replacing $m_\pi \rightarrow m_K$. We use $M_A = 1.23 \text{ GeV} \simeq \sqrt{2}M_\rho$ because of Weinberg's sum rules [66] and the KSFR relation [67]. We do not coincide with the expression given in ref.[65] (also employed in ref.[18]) for $T_{A, \pi^+\pi^-}$. However, we do agree with the formula given in ref.[14] for the similar exchange of the 1^{+-} axial-vector resonances, that has the same Lorentz structure. In ref.[65] the authors perform the check that at $\mathcal{O}(p^4)$ they reproduce the χ PT result for $\gamma\gamma \rightarrow \pi^+\pi^-$. This implies the axial-vector saturation of the chiral counterterm $L_9 + L_{10}$,

$$L_9 + L_{10} = \frac{F_A^2}{4M_A^2} . \quad (3.25)$$

We also fulfill this condition since at $\mathcal{O}(p^4)$ our expression is $T_{A, \pi^+\pi^-} = 2e^2 \frac{F_A^2}{M_A^2 f_\pi^2} (k_1 k_2)(\epsilon_1\epsilon_2) + \mathcal{O}(p^6)$ and agrees with that of ref.[11] if eq.(3.25) is taking into account. We use eq.(3.25) to fix F_A from the value $L_9 + L_{10} = (1.4 \pm 0.3) \cdot 10^{-3}$. In the following we shall replace F_A^2 by $L_9 + L_{10}$ using eq.(3.25). In ref.[68] the couplings of the vector and axial-vector resonances to pseudoscalars and external sources are calculated within the Extended Nambu-Jona-Laisinio model [69].

The S-wave projection of eq.(3.24) is,

$$T_{A,P\bar{P}}^S = 2e^2 \frac{L_9 + L_{10}}{f_\pi^2} \left[\frac{M_A^2}{\sigma_P} \log \frac{1 + \sigma_P + s_A/s}{1 - \sigma_P + s_A/s} + s \right], \quad (3.26)$$

with $P = \pi^+, K^+$ and $s_A = 2(M_A^2 - m_P^2)$. This equation differs with the S-wave projection of ref.[18], that employs the results of ref.[65] which disagree with our eq.(3.24). While we have the coefficient M_A^2 in front of the logarithm, ref.[18] has $s_A/2$. This mistake was also performed in ref.[19], because the expression from ref.[18] was taken. In addition, we have also included now the exchange of the K^* vector resonance, not taken into account in ref.[19]. The numerical differences of correcting for these latter deficiencies are however very small.

We finally give the expressions for the exchange of the 1^{+-} nonet of axial-vector resonances. We make use of the lowest order Lagrangian, see e.g. ref.[14],

$$\mathcal{L} = \frac{eD}{f_\pi} F_{\mu\nu} \langle \bar{C}^\mu \{Q, \partial^\nu \Phi\} \rangle, \quad (3.27)$$

where $C_\mu = \frac{1}{\sqrt{2}} C_\mu^i \lambda^i + \frac{1}{\sqrt{3}} C_\mu^9 \cdot \mathbf{1}$, with standard notation. We then have,

$$T_{C,P\bar{P}} = \frac{e^2 D^2}{18 f_\pi^2} \ell_P \left[\frac{(\epsilon_1 \epsilon_2)(t - m_P^2)^2 - 2s(\epsilon_1 p_1)(\epsilon_2 p_1)}{t - M_C^2} + \frac{(\epsilon_1 \epsilon_2)(u - m_P^2)^2 - 2s(\epsilon_1 p_1)(\epsilon_2 p_1)}{u - M_C^2} \right], \quad (3.28)$$

with $\ell_{\pi^0} = 5$, $\ell_{\pi^+} = 1/2$, $\ell_{K^+} = 1/2$ and $\ell_{K^0} = 2$. The S-wave projection is

$$T_{C,P\bar{P}}^S = -\frac{e^2 D^2}{18 f_\pi^2} \ell_P \left[s + \frac{M_C^2}{\sigma_P} \log \frac{1 - \sigma_P + s_C/s}{1 + \sigma_P + s_C/s} \right]. \quad (3.29)$$

We take for $M_C = 1.23$ GeV, the value corresponding to the mass of the $b_1(1235)$ resonance. The constant D is determined from the $b_1 \rightarrow \gamma\pi^+$ decay [70],

$$D^2 = \frac{M_C^3 \Gamma(b_1 \rightarrow \gamma\pi^+) 216 f_\pi^2}{(M_C^2 - m_\pi^2)^3 \alpha} \simeq 3.2 \cdot 10^{-2}. \quad (3.30)$$

3.2 Isospin amplitudes

Here we present our isospin amplitudes for $\gamma\gamma \rightarrow (\pi\pi)_I$. We employ the isospin states,

$$\begin{aligned} |\pi\pi\rangle_0 &= \frac{-1}{\sqrt{3}} |\pi^+\pi^- + \pi^-\pi^+ + \pi^0\pi^0\rangle, \\ |\pi\pi\rangle_2 &= \frac{-1}{\sqrt{6}} |\pi^+\pi^- + \pi^-\pi^+ - 2\pi^0\pi^0\rangle, \end{aligned} \quad (3.31)$$

with the subscript indicating the corresponding isospin. As a result, for the S-wave of $\gamma\gamma \rightarrow (\pi\pi)_I$

$$\begin{aligned} T_{\gamma\gamma,0}^S &= -\frac{2}{\sqrt{3}} \left(T_{\pi^+\pi^-}^S + \frac{1}{2} T_{\pi^0\pi^0}^S \right), \\ T_{\gamma\gamma,2}^S &= -\sqrt{\frac{2}{3}} \left(T_{\pi^+\pi^-}^S - T_{\pi^0\pi^0}^S \right). \end{aligned} \quad (3.32)$$

This isospin decomposition applies not only to the whole S-wave amplitude but to all of its partial contributions, Born term, vector and axial exchanges, etc.

4 Results

In this section we discuss about the results that follow from the use of the dispersive and dynamical approaches, sections 2 and 3, respectively.

4.1 Determination of the constants in the dispersive method

Let us first consider the dispersive approach. The $L_I(s)$ functions have contributions from the Born term and from the vector and axial-vector crossed exchanges:

$$\begin{aligned} L_0 &= -\frac{2}{\sqrt{3}}T_B^S - \frac{2}{\sqrt{3}}T_{A,\pi\pi}^S - \sqrt{3}T_{\rho,\pi\pi}^S - \frac{1}{\sqrt{3}}T_{\omega,\pi\pi}^S + \frac{1}{3\sqrt{3}}T_{C,\pi\pi}^S, \\ L_2 &= -\sqrt{\frac{2}{3}}\left(T_B^S + T_{A,\pi\pi}^S - T_{\omega,\pi\pi}^S + \frac{1}{4}T_{C,\pi\pi}^S\right), \end{aligned} \quad (4.33)$$

where

$$T_{C,\pi\pi} = \frac{e^2 D^2}{f_\pi^2} \left[s + \frac{M_C^2}{\sigma_\pi} \log \frac{1 - \sigma_\pi + s_C/s}{1 + \sigma_\pi + s_A/s} \right]. \quad (4.34)$$

We now turn to the coefficients c_0 and c_2 of eq.(2.4). As discussed in section 2 these coefficients are determined by matching with the χPT one loop results for the linear behaviour in s of $F_C(s) - B_C(s)$ and $F_N(s)$ when $s \rightarrow 0$. In order to impose the condition **1** one should realize that only $T_{A,\pi^+\pi^-}^S$ is $\mathcal{O}(s)$, being all the other resonance exchanges $\mathcal{O}(s^2)$. Then,

$$F_C(s) = T_B^S + 4e^2\chi \frac{L_9 + L_{10}}{f_\pi^2} s - \frac{c_0 s}{\sqrt{3}} - \frac{c_2 s}{\sqrt{6}} + \mathcal{O}(s^2), \quad (4.35)$$

where $\chi = (1 - m_\pi^2/2M_A^2)/(1 - m_\pi^2/M_A^2)$. The one loop χPT result is

$$F_C(s) = T_B^S + 4e^2 \frac{L_9 + L_{10}}{f_\pi^2} s + \mathcal{O}(s^2), \quad (4.36)$$

and it follows that

$$c_0 + \frac{1}{\sqrt{2}}c_2 = \xi \quad (4.37)$$

with

$$\xi = 4\sqrt{3}e^2 \frac{L_9 + L_{10}}{f_\pi^2} (\chi - 1). \quad (4.38)$$

Notice that χ is very close to one and then $\xi \simeq 0$

Regarding the condition **2**, the linear dependence in s of $F_N(s)$ around $s = 0$ from eq.(2.4) is given by

$$F_N(s) = -\frac{1}{\sqrt{3}}c_0 s + \sqrt{\frac{2}{3}}c_2 s + \mathcal{O}(s^2). \quad (4.39)$$

One loop χPT establishes that

$$F_N^S(s) = -e^2 s/96\pi^2 f_\pi^2 + \mathcal{O}(s^2), \quad (4.40)$$

so that

$$\begin{aligned}
c_0 &= \frac{e^2 \sqrt{1/3}}{96\pi^2 f_\pi^2} + \frac{2}{3}\xi, \\
c_2 &= -\frac{e^2 \sqrt{2/3}}{96\pi^2 f_\pi^2} + \frac{\sqrt{2}}{3}\xi.
\end{aligned}
\tag{4.41}$$

We evaluate the previous expressions given by one loop χ PT either by employing $f_\pi = 92.4$ MeV or $f \simeq 0.94f_\pi$, where the former is the pion decay constant and the latter is the same but in the $SU(2)$ chiral limit [7]. This amounts around a 12% of uncertainty in the evaluation of c_0 and c_2 , due to the square dependence on f_π . Note that both choices, f_π or f , are consistent with the precision of the one loop calculation and the variation in the results is an estimate for higher orders corrections. This is included in the error analysis.

The constant $F_0(s_1) - L_0(s_1)$ in eq.(2.4) is related with the position of the Adler zero s_A , where $F_N(s_A) = 0$, by

$$\begin{aligned}
\frac{\omega_0(s_A)}{\omega_0(s_1)} \frac{s_A^2}{s_1^2} [F_0(s_1) - L_0(s_1)] &= \sqrt{2}L_2(s_A) - L_0(s_A) + \left(\sqrt{2}c_2\Omega_2(s_A) - c_0\Omega_0(s_A) \right) s_A \\
&+ \sqrt{2} \frac{s_A^2}{\pi} \Omega_2(s_A) \int_{4m_\pi^2}^{\infty} \frac{L_2(s') \sin \phi_2(s') ds'}{s'^2(s' - s_A) |\Omega_2(s')|} \\
&- \frac{s_A^2}{\pi} \Omega_0(s_A) \int_{4m_\pi^2}^{\infty} \frac{L_0(s') \sin \bar{\phi}_0(s') ds'}{s'^2(s' - s_A) |\Omega_0(s')|}.
\end{aligned}
\tag{4.42}$$

As discussed in the condition **3** of sec.2 the value of $F_0(s_1) - L_0(s_1)$ is finally fixed by requiring that $\sigma(\gamma\gamma \rightarrow \pi^0\pi^0) \leq 40$ nb at the $f_0(980)$ peak, at $\simeq s_1$. This is based on the experimental data for $\gamma\gamma \rightarrow \pi^0\pi^0$ of ref.[13], see fig.7 where the data including the $f_0(980)$ are shown, whose maximum value at the $f_0(980)$ peak of $\sigma(\gamma\gamma \rightarrow \pi^0\pi^0) < 40$ nb, errors included. In addition, we also take into account the resulting width $\Gamma(f_0(980) \rightarrow \gamma\gamma) = 205_{-83}^{+95}(\text{stat})_{-117}^{+147}(\text{sys})$ eV from the Belle Collaboration [31], and then impose that the width calculated from our approach lies within the interval 60-380 eV, as follows from the previous value. This interval is compatible with the one recently given for the width $\Gamma(f_0(980) \rightarrow \gamma\gamma)$ in ref.[71] and with the value $\Gamma(f_0(980) \rightarrow \gamma\gamma) = 0.2$ KeV predicted by the dynamical approach [19]. Note that $\Gamma(f_0(980) \rightarrow \gamma\gamma)$ is proportional to the maximum value of $\sigma(\gamma\gamma \rightarrow \pi^0\pi^0)$ at the $f_0(980)$ peak. For practical purposes both constraints are equivalent.

4.2 The $\gamma\gamma \rightarrow \pi^0\pi^0$ cross section

In our normalization, the cross section in terms of $F_N(s)$ is given by

$$\sigma(\gamma\gamma \rightarrow \pi^0\pi^0) = \frac{\sigma_\pi}{64\pi s} |F_N(s)|^2.
\tag{4.43}$$

Since the main contribution in the low energy region to $\Omega_I(s)$ comes from the low energy $\pi\pi$ phase shifts one needs to be rather precise for the input parameterizations of the $\pi\pi$ scattering data in this energy region in order to apply the dispersive method, eqs.(2.2) and (2.4). The small

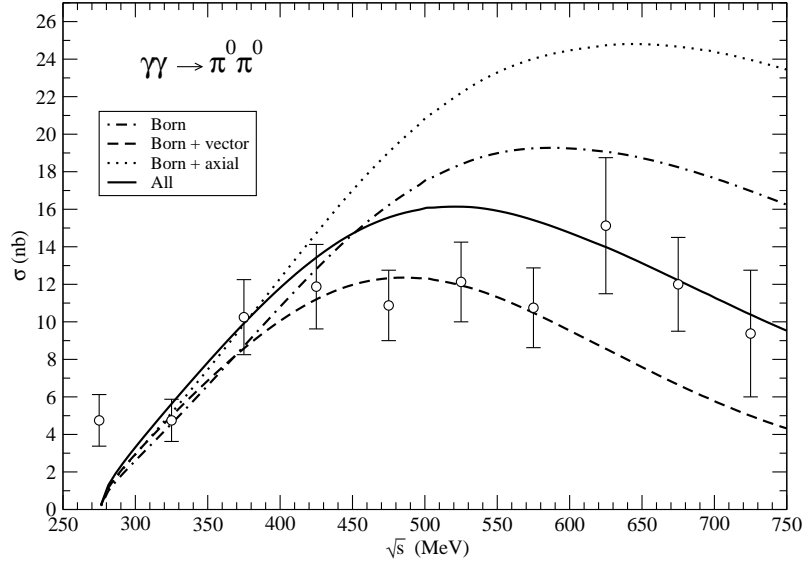


Figure 4: The $\gamma\gamma \rightarrow \pi^0\pi^0$ cross section depending on the contributions included for $L_I(s)$. Dot-dashed line (Born term only), dashed line (Born term plus vector crossed exchanges) and dotted line (Born term plus axial-vector crossed exchange mechanisms). The solid line is the full result.

$I = 2$ S-wave $\pi\pi$ phase shifts, which induce small final state interaction corrections anyhow, can be parameterized in simple terms and our fit compared to data can be seen in fig.2. For $I = 0$ one of the parameterizations that we consider is the K-matrix of Hyams *et. al.* [52],

$$K_{ij}(s) = \alpha_i\alpha_j/(x_1 - s) + \beta_i\beta_j/(x_2 - s) + \gamma_{ij} , \quad (4.44)$$

where

$$\begin{aligned} x_1^{1/2} &= 0.11 \pm 0.15 & x_2^{1/2} &= 1.19 \pm 0.01 \\ \alpha_1 &= 2.28 \pm 0.08 & \alpha_2 &= 2.02 \pm 0.11 \\ \beta_1 &= -1.00 \pm 0.03 & \beta_2 &= 0.47 \pm 0.05 \\ \gamma_{11} &= 2.86 \pm 0.15 & \gamma_{12} &= 1.85 \pm 0.18 & \gamma_{22} &= 1.00 \pm 0.53 , \end{aligned} \quad (4.45)$$

in units of appropriate powers of GeV. The K matrix is related to the $I = 0$ S-wave T -matrix by

$$T = -8\pi\sqrt{s}(K^{-1} - iQ)^{-1} , \quad (4.46)$$

where $Q = \text{diag}(q_\pi, q_K)$ with $q_\pi(q_K)$ the center of mass momentum of the pions (kaons). The central values in eq.(4.45) correspond to $\delta_\pi(s_K)_0 < \pi$. However, varying the parameters within their errors it is possible to obtain $\delta_\pi(s_K)_0 > \pi$ (see fig.2 where both cases are shown). Since below 0.6 GeV this K-matrix was not fitted to data and strongly disagrees with K_{e4} data [55, 56], we consider instead the parameterizations of ref.[59] (CGL), ref.[60] (PY) and ref.[10] (AO). They agree with data from K_{e4} decays [55, 56] and span to a large extent the band of theoretical uncertainties in the $I = 0$ S-wave $\pi\pi$ phase shifts [52–54]. PY runs through the higher values of $\delta_\pi(s)_0$, while CGL does through lower values, see fig.2. AO, double-dash-dotted line, moves somewhat in between the previous results for energies between 0.5-0.7 GeV and then follows closely

CGL results. CGL is used up to 0.8 GeV, since this is the upper limit of its analysis, and the K-matrix eq.(4.44) above that energy. On the other hand, PY is employed up to 0.9 GeV, as in this energy this parameterization agrees well inside errors with [52], and eq.(4.44) above it. AO is used up to 1.5 GeV since it fits S-wave meson-meson data up to 2 GeV. We shall also employ in some cases the results for the $\pi\pi$ phase shifts from ref. [1], which gives rise to a $f_0(980)$ signal tested in many other processes like e.g. J/Ψ [50, 72], D [73] and ϕ [20, 74] decays. This parameterization will be referred in the following as OO and will be used in the region $0.9 \leq \sqrt{s} \leq 1.1$ GeV, above it eq.(4.44) is again taken and below CGL.

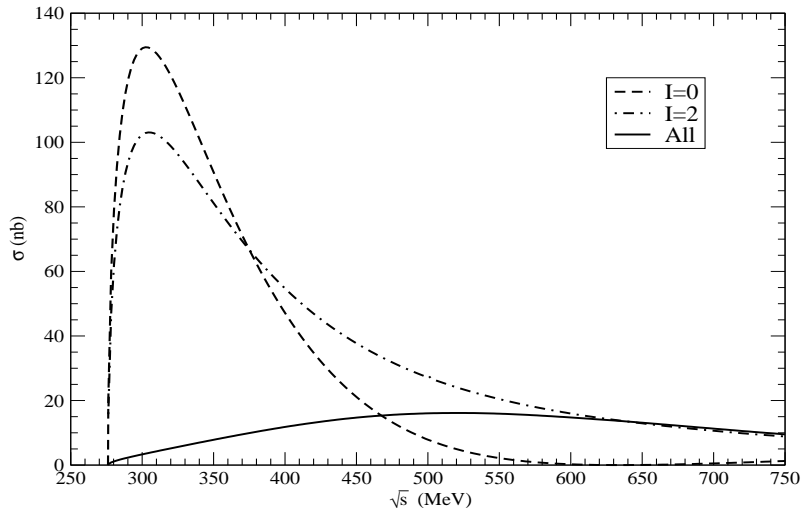


Figure 5: $I = 0$ (dashed) and 2 (dot-dashed) contributions to the $\gamma\gamma \rightarrow \pi^0\pi^0$ cross section. The solid line is the full result. The curves have been generated employing the parameterizations CGL and Hyams [52].

In fig.4 we show the different contributions to the $\gamma\gamma \rightarrow \pi^0\pi^0$ cross section compared with data^{#3} [13]. The different curves originate by considering only the Born term as the only contribution to $L_I(s)$ in eq.(2.4) (dot-dashed line), the Born term and the exchanges of vector resonances (dashed line), the Born term and the exchanges of axial-vector resonances (dotted line) and the full model (solid line) for L_I , i.e., the Born term plus vector and axial-vector resonance exchanges. The curves have been evaluated with the central values of the parameterizations eq.(4.44) and CGL. One can see that the dominant contribution comes from the dressing of the Born term by final state interactions, despite that the Born term at tree level is zero. The vector and axial-vector resonance exchange mechanisms also give important contributions to the total cross section, even already at threshold for the exchange of the axial-vector resonances. Most of the vector resonance crossed exchange contribution comes from the ω exchange, since the ω coupling to $\gamma\pi^0$ is about one order of magnitude larger than that due to the ρ or K^* resonances. It is clear from the figure that the axial-vector meson exchange mechanisms, overlooked in refs.[26, 28], are found to be substantial and tend to increase the cross section. Notice that the cross section given in ref.[26] is very close to the dashed line in fig.4.

^{#3}Since the data only cover up to $|\cos\theta| < Z$, with $Z = 0.8$, we have divided them by the factor Z . This suited for low energies as S-wave dominates, for higher energies is a normalization convention.

It is also worth stressing that there are strong interferences between the different mechanisms, as well as between the isospin $I = 0$ and $I = 2$ amplitudes. In fig.5, we show the $\gamma\gamma \rightarrow \pi^0\pi^0$ cross section considering only the $I = 0$ S-wave contribution (dashed line), the $I = 2$ S-wave contribution (dot-dashed line) and the full result (solid line). For definiteness, the curves are calculated with the central value of ref.[52] and CGL for low energies. We can see the strong cancellation between the $I = 0$ and $I = 2$ contributions due to the absence of the Born term at tree level in the $\gamma\gamma \rightarrow \pi^0\pi^0$ channel, which is the dominant contribution in the $I = 0$ and $I = 2$ channels. The Born term is the responsible in every isospin channel for the bumps at low energies in fig.5, though the strong final state interactions in $I = 0$ reshapes it considerably and tends to accumulate strength to lower energies than for the $I = 2$ part.

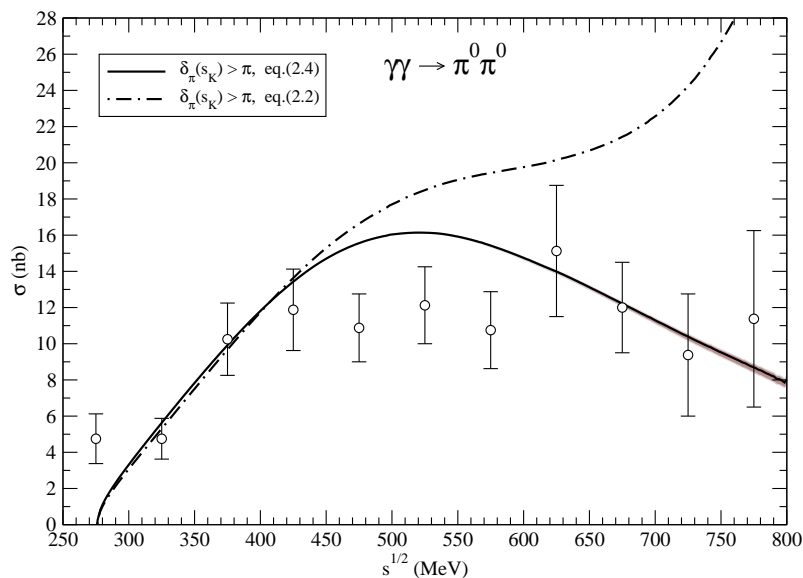


Figure 6: The error band around the solid line is the uncertainty in our results by requiring that $\sigma(\gamma\gamma \rightarrow \pi^0\pi^0) \lesssim 40$ nb at s_1 . The solid line should be compared with the dot-dashed one, that would correspond to the formalism of ref.[26] in the case that $\phi_0(s) \simeq \delta_\pi(s)_0$ above s_K and including the axial-vector exchanges. The lines are evaluated with the central values of CGL and eq.(4.44).

In fig.6 we show with the solid line our results for the central values of eq.(4.44) and CGL while the dashed-solid line corresponds to the result that would be obtained if using the approach of ref.[26] (including also the axial-vector exchanges). The improvement achieved by passing from the dot-dashed line to the solid one is determined by using eq.(2.4) instead of eq.(2.2), being the latter the original equation derived in refs.[26–28]. The gray band around the solid line corresponds to the uncertainty originated exclusively by taking $\sigma(\gamma\gamma \rightarrow \pi^0\pi^0) \leq 40$ nb at s_1 .

We include in fig.7 the $f_0(980)$ region as well, plotting for $\sqrt{s} \leq 1.05$ GeV. The generation of the $f_0(980)$ resonance peak within the dispersive method is a remarkable achievement with important consequences as it has been used already for fixing that the $z = +1$ behaviour of $\phi_0(s)$ is the one realized in nature. We have also used it to constraint the values of $F_0(s_1) - L_0(s_1)$, so that we are able to take three subtractions in the dispersion relation instead of just two, as in previous studies. The values of $F_0(s_1) - L_0(s_1)$ are fixed in this figure such that the size of

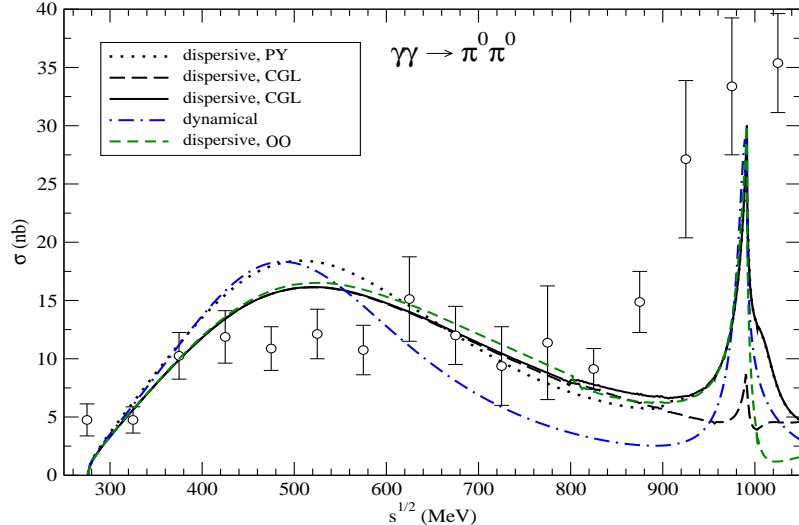


Figure 7: The $\sigma(\gamma\gamma \rightarrow \pi^0\pi^0)$ cross section including the region of the $f_0(980)$. We show two different curves such that the cross section at the top of the peak is 10 and 30 nb, long-dashed and solid lines, respectively. The short-dashed line employs the OO parameterization around the $f_0(980)$ resonance. The dot-dashed line is evaluated with the dynamical method of ref.[19].

$\sigma(\gamma\gamma \rightarrow \pi^0\pi^0)$ in the $f_0(980)$ peak is 10 or 30 nb, dashed and solid lines, respectively. These lines are evaluated with the central values of CGL and eq.(4.44) for definiteness. From this figure it is clear that above ~ 0.8 GeV the D-wave contribution in $\sigma(\gamma\gamma \rightarrow \pi^0\pi^0)$, due to the tail of the $f_2(1270)$, is important and this resonance is needed so as to agree width data. This contribution is added incoherently because of the azimuthal integration (the $f_2(1270)$ resonance signal in $\gamma\gamma$ has dominantly helicity 2 [27]). We also show in the figure by the short-dashed line the result from the dispersive approach but employing the parameterization OO for the $\pi\pi$ phase shifts around the $f_0(980)$ resonance. The dot-dashed line is calculated with the dynamical method of ref.[19]. This method rightly predicts the peak at 0.5 GeV, with size very similar to that obtained from the dispersive method and using PY, though tends to give somewhat a too fast decreasing cross section for energies above $\gtrsim 0.6$ GeV. In fig.9 we also show the curve corresponding to the AO parameterization with a peak value in the $f_0(980)$ of 20 nb. In this way one can see how the actual shape of the $f_0(980)$ signal changes depending on the parameterizations and on the peak values used. Further theoretical precision in this energy region requires to include the D-wave $\gamma\gamma \rightarrow \pi\pi$ contribution and fit simultaneously the recent data on $\gamma\gamma \rightarrow \pi^+\pi^-$ [31]. This is beyond the scope of the present study.

Our final $\sigma(\gamma\gamma \rightarrow \pi^0\pi^0)$ for $\sqrt{s} < 0.8$ GeV is shown in fig.8. We give the results for CGL(solid) and PY(dashed) and eq.(4.44), as usual. The corresponding band around the lines has into account all the theoretical uncertainties discussed with respect to the dispersive approach. For that, we implement a Monte-Carlo Gaussian sampling taking into account the errorbars in the parameters of CGL, PY and eq.(4.44), the uncertainty for $s > s_K$ in the approximation $\phi_0(s) \simeq \delta_\pi(s)_0$ in the region $1 \lesssim \sqrt{s} \lesssim 1.5$ GeV and that from eq.(2.13) above s_H . We also include in the error the 12% uncertainty in evaluating c_0 and c_2 according to eq.(4.41) and the variation within the

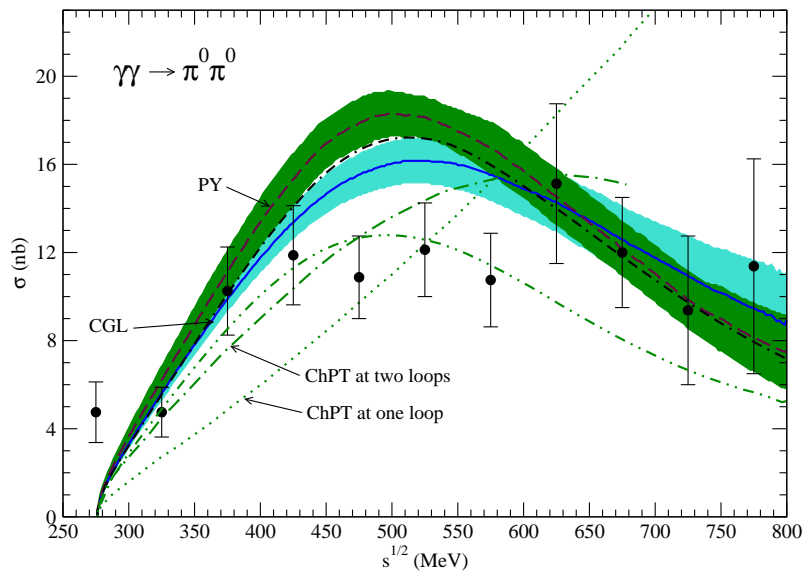


Figure 8: Final result for the $\gamma\gamma \rightarrow \pi^0\pi^0$ cross section with the theoretical error band. The experimental data are from the Crystal Ball Collaboration ref.[13]. The dashed line is evaluated with PY and the solid line with CGL. The band around each line corresponds to the theoretical uncertainties. The dot-dashed line corresponds to AO and does not include error band, of similar size than the ones shown, in order not to overload the figure.

bound $\sigma(\gamma\gamma \rightarrow \pi^0\pi^0) \leq 40$ nb at s_1 . The width of the band is dominated by the errors in the parameterizations PY and CGL. In the same figure the dark dot-dashed line corresponds to the AO phase shifts. We do not show its corresponding error bar as it is of similar size as for CGL and PY and it would complicate the visualization of the information contained in the figure. In addition, the dotted line corresponds to one loop CHPT [11, 12] and the lighter dot-dashed one is the two loop result [14, 15]. The latter is closer to the dispersive results for low energies but still one observes that the $\mathcal{O}(p^8)$ corrections would be sizable. It is worth stressing that if the axial-vector exchanges were removed, in refs.[26, 28] they were not included, then our curves would be smaller. This corresponds to the dot-dot-dashed line in fig.8, which is very close to that of ref.[26] when employing $\phi_0(s) \simeq \delta_\pi(s)_0 - \pi$ for $s > s_K$. The former curve is evaluated making use of CGL and ref.[52] with their central values. The three experimental points [13] in the region 0.45-0.6 GeV agree well with this curve. However, once the axial-vector are included the curve rises. These three points lie around 1.5σ below the CGL result band, and by somewhat more than two sigmas below the PY band. This clearly shows that more precise experimental data on $\gamma\gamma \rightarrow \pi^0\pi^0$ could be used to distinguish between different low-energy parameterizations of the $I = 0$ $\pi\pi$ S-wave phase shifts. The next three experimental points in the region 0.6-0.75 GeV agree better when the axial-vector resonance contributions are taken into account, as one should do. As a result of this discussion, more precise experimental data for $\gamma\gamma \rightarrow \pi^0\pi^0$ are called for. The width of the error bands around the solid and dashed lines is reduced as compared with ref.[29] because now the $z = +1$ case has been singled out.

In fig.9 we show our final results for $\sigma(\gamma\gamma \rightarrow \pi^0\pi^0)$ including the $f_0(980)$ region as well. The error bands are evaluated similarly as for fig.8. One appreciates how the widths of the error bands

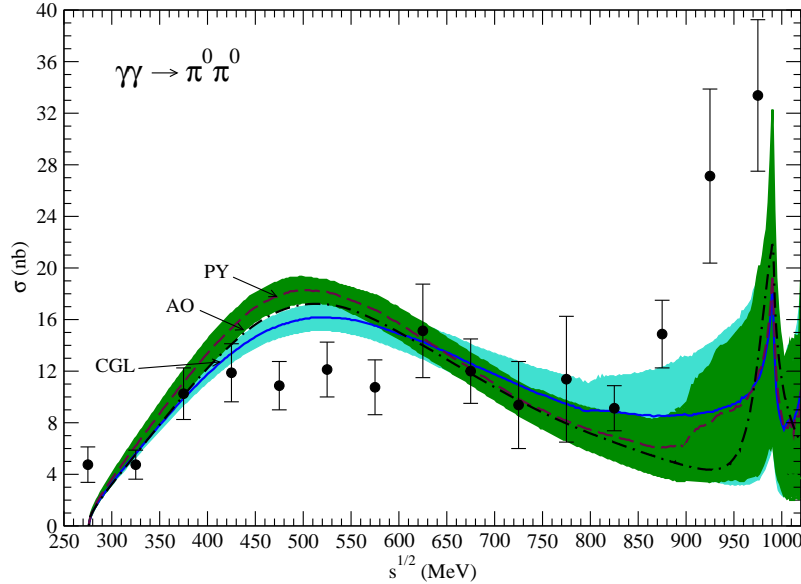


Figure 9: Final result for the $\gamma\gamma \rightarrow \pi^0\pi^0$ cross for $\sqrt{s} \leq 1.05$ GeV. The experimental data are from the Crystal Ball Collaboration ref.[13]. The dashed line is evaluated with PY and the solid line with CGL. The band around each line corresponds to the theoretical uncertainties. The dot-dashed line correspond to using AO. Its error band, not shown, is similar to the ones of the other two curves.

largely increase in the $f_0(980)$ region because of the uncertainty in the input for the value at the peak $4 \leq \sigma(\gamma\gamma \rightarrow \pi^0\pi^0) \leq 40$ nb, which is obtained by requiring that $\Gamma(f_0(980) \rightarrow \gamma\gamma)$, as calculated from our approach, lies in the range of the value determined in ref.[31], $\Gamma(f_0(980) \rightarrow \gamma\gamma) = 205_{-83}^{+95}(\text{stat})_{-117}^{+147}(\text{sys})$ eV. This bound in the size of the $f_0(980)$ peak could be also inferred by simple inspection of the experimental data in the same figure since otherwise the $f_0(980)$ peak would be larger than the total cross-section, which also includes incoherently a large D-wave contribution from the tail of the $f_2(1270)$. A reduction of this uncertainty in the $f_0(980)$ has to await a proper study of the new data $\gamma\gamma \rightarrow \pi^+\pi^-$ [31] along these lines, as already commented.

From our approach we obtain that the Adler zero in $F_N(s)$ is located at $s_A = (1.11 \pm 0.03) m_\pi^2$, if CGL is used, and at $s_A = (1.09 \pm 0.04) m_\pi^2$, when PY is taken for lower energies. If AO is used up to 1.4 GeV we obtain for s_A the same value as the latter one. From our analysis then s_A lies in the range $(1.05-1.14) m_\pi^2$. This range is in agreement with the the two loop χ PT value [14], $s_A = 1.175 m_\pi^2$. The difference is around a 4%, well inside the expected uncertainties of ref.[14].

4.3 The $\sigma \rightarrow \gamma\gamma$ width

Let us recall that the σ is the lightest resonance with the quantum numbers of the vacuum. It was originally included by studies of the NN potential, but due to the advent of the chiral potentials [75–77] it is no longer necessary and, furthermore, chiral symmetry seems to substantially reduce its contributions [78]. Another relevant example where the σ is introduced is the linear sigma model [79]. However, when the non-linear sigma models are unitarized, fulfilling the unitarity and analyticity requirements associated with the right hand cut, a pole associated with the σ resonance appears as well [1–5, 80]. The works [1, 3] were the first to show that the presence of

such a light scalar resonance is not in contradiction with the non-linear sigma models. It appears because of the strong interactions, driven by chiral symmetry, between the two pions in an $I = 0$ S-wave pair. In ref.[81] it was shown that in the limit of chiral symmetry restoration, $f_\pi \rightarrow 0$, the σ pole moves to zero and becomes the chiral partner of the pion. In this respect, the difference in mass between the σ resonance and the π is an order parameter for chiral symmetry breaking. It is interesting to consider the σ coupling to $\gamma\gamma$ because, as indicated in the Introduction, it is a complementary information apart from that of scattering as it is sensitive to the electric charge. This can give clues to possible underlying structures in its nature.

For the evaluation of the coupling $\sigma \rightarrow \gamma\gamma$, $g_{\sigma\gamma\gamma}$, the amplitude $F_N(s)$ has to be evaluated not on the first or physical Riemann sheet but on the second one. This is accomplished by shifting $q_\pi \rightarrow -q_\pi$. We denote by $\tilde{F}_N(s)$ the resulting amplitude on the second Riemann sheet. The strong $I = 0$ $\pi\pi$ S-wave T -matrix on the same sheet, $T_{II}(s)$, can be calculated in terms of the one on the physical sheet, $T_I(s)$, by

$$T_{II}^{-1} = T_I^{-1} - i \frac{q_\pi}{4\pi\sqrt{s}}. \quad (4.47)$$

T_{II} and \tilde{F}_N have a pole corresponding to the σ resonance at s_σ , so that

$$\lim_{s \rightarrow s_\sigma} \tilde{F}_N^S = \frac{g_{\sigma\gamma\gamma} g_{\sigma\pi^0\pi^0}}{s_\sigma - s}, \quad (4.48)$$

where $g_{\sigma\pi^0\pi^0}$ is the coupling of the σ to $\pi^0\pi^0$.^{#4}

From F_N of eq.(3.14), corresponding to the extended dynamical approach of ref.[19], the coupling $g_{\sigma\gamma\gamma}$ is

$$\begin{aligned} g_{\sigma\gamma\gamma} &= \sqrt{\frac{2}{3}}(\tilde{t}_{A\pi^+\pi^-} + 1.1\tilde{t}_{C\pi^0\pi^0} + \tilde{t}_{\omega\pi^0\pi^0} + 2\tilde{t}_{\rho\pi^+\pi^-} + \tilde{t}_{\chi\pi})g_{\sigma\pi\pi} \\ &+ \frac{1}{\sqrt{2}}(\tilde{t}_{AK^+K^-} + 5\tilde{t}_{CK^+K^-} + 2\tilde{t}_{K^*K^+K^-} + \tilde{t}_{\chi K})g_{\sigma K\bar{K}} \\ &= g_{\sigma\pi\pi} \left[\sqrt{\frac{2}{3}}(\tilde{t}_{A\pi^+\pi^-} + 1.1\tilde{t}_{C\pi^0\pi^0} + \tilde{t}_{\omega\pi^0\pi^0} + 2\tilde{t}_{\rho\pi^+\pi^-} + \tilde{t}_{\chi\pi}) \right. \\ &\left. + \frac{1}{\sqrt{2}}(\tilde{t}_{AK^+K^-} + 5\tilde{t}_{CK^+K^-} + 2\tilde{t}_{K^*K^+K^-} + \tilde{t}_{\chi K}) \frac{g_{\sigma K\bar{K}}}{g_{\sigma\pi\pi}} \right] \end{aligned} \quad (4.49)$$

In the previous equation $g_{\sigma\pi\pi}$ is the coupling of the σ to the $I = 0$ $\pi\pi$ state in the unitary normalization of refs.[19, 80]^{#5} and, analogously, $g_{\sigma K\bar{K}}$ is the coupling to the $I = 0$ $K\bar{K}$ one. Notice that the ratio of couplings is given directly by $g_{\sigma K\bar{K}}/g_{\sigma\pi\pi} = t_{K\bar{K},K\bar{K}}^0/t_{\pi\pi,K\bar{K}}^0$, with the strong amplitudes evaluated on the second Riemann sheet.

It is important to remark that the ratio $g_{\sigma\gamma\gamma}/g_{\sigma\pi\pi}$ does not depend^{#6} on the strong meson-meson coupling, hence it allows a clearer comparison between different approaches for the $\gamma\gamma \rightarrow \pi\pi$ part.

^{#4}As it is well known [82] the phase of a resonance coupling is background dependent. Hence, the phase of $g_{\sigma\pi^0\pi^0}$ extracted from $\gamma\gamma \rightarrow \pi^0\pi^0$ differs from that obtained, e.g., from $\pi^0\pi^0 \rightarrow \pi^0\pi^0$. This does not bother us here since we are only interested in the moduli of $g_{\sigma\gamma\gamma}$ and $g_{\sigma\pi^0\pi^0}$.

^{#5}With the unitarity normalization the width to $\pi\pi$ of an $I = 0$ narrow resonance of mass M is given by $\Gamma = |g_{\sigma\pi\pi}|^2 q_\pi / (8\pi M^2)$.

^{#6}Actually there is a dependence from eq.(4.49) on the strong coupling due to the kaons, but this term is very small numerically.

We now determine $g_{\sigma\gamma\gamma}/g_{\sigma\pi\pi}$ and $\Gamma_{\sigma\rightarrow\gamma\gamma}$ by using the dispersive approach of section 2. The dispersion relation eq.(2.4) to calculate $F_0(s)$ is only valid on the first Riemann sheet. If evaluated on the second Riemann sheet there would be an extra term due to the σ pole. However, the relation between F_0 and \tilde{F}_0 , the latter on the second sheet, can be easily established using unitarity above the $\pi\pi$ threshold,

$$F_0(s+i\epsilon) - F_0(s-i\epsilon) = -2iF_0(s+i\epsilon)\rho(s+i\epsilon)T_{II}^0(s-i\epsilon), \quad (4.50)$$

with $4m_\pi^2 < s < 4m_K^2$, $\rho(s) = \sigma_\pi(s)/16\pi$ and $\epsilon \rightarrow 0^+$. Due to the continuity when changing from one sheet to the other,

$$F_0(s-i\epsilon) = \tilde{F}_0(s+i\epsilon), \quad T_{II}^{I=0}(s-i\epsilon) = T_{II}^{I=0}(s+i\epsilon). \quad (4.51)$$

it results then from eq.(4.50)

$$\tilde{F}_0(s) = F_0(s) (1 + 2i\rho(s)T_{II}^{I=0}(s)), \quad (4.52)$$

where the analytical extrapolation of eqs.(4.50) and eq.(4.51) has been taken. Around the σ pole,

$$T_{II}^{I=0} = -\frac{g_{\sigma\pi\pi}^2}{s_\sigma - s}, \quad \tilde{F}_0(s) = \sqrt{2} \frac{g_{\sigma\gamma\gamma}g_{\sigma\pi\pi}}{s_\sigma - s}, \quad (4.53)$$

and then from eq.(4.52)

$$g_{\sigma\gamma\gamma}^2 = -g_{\sigma\pi\pi}^2 \frac{1}{2} \left(\frac{\sigma_\pi(s_\sigma)}{8\pi} \right)^2 F_0(s_\sigma)^2. \quad (4.54)$$

This expression allows to evaluate again the ratio $g_{\sigma\gamma\gamma}/g_{\sigma\pi\pi}$.

We consider in the subsequent $s_\sigma = (M_\sigma - i\Gamma_\sigma/2)^2$ either from the studies of ref.[10] or ref.[8]. The former provides a reproduction of the S-wave $I = 0$ and $K^-\pi^+ \rightarrow K^-\pi^+$ data from $\pi\pi$ threshold up to around 2 GeV, considering for the first time 13 coupled channels for the $I = 0$ meson-meson S-wave. The interactions kernels are derived from chiral Lagrangians and are unitarized employing the N/D method [2]. Multiparticle states are mimicked by $\sigma\sigma$, $\rho\rho$, $\omega\omega$, \dots . The $\sigma\sigma$ elementary transition amplitudes are given without any new free parameter, the same as for the vector-vector ones which are derived by making use of a massive Yang-Mills theory [83]. In ref.[10] one has $M_\sigma^{AO} = (456 \pm 6)$ MeV and $\Gamma_\sigma^{AO} = (482 \pm 20)$ MeV. Ref.[8] provides the values $M_\sigma^{CCL} = 441_{-8}^{+16}$ MeV and $\Gamma_\sigma^{CCL} = 544_{-25}^{+18}$ MeV. The latter values result from the $I = 0$ $\pi\pi$ S-wave amplitude obtained after solving the Roy equations and matching with CHPT to two loops. In the following the superscripts *AO* and *CCL* refer to those results obtained by employing s_σ from ref.[10] or [8], respectively.

In table 1 we give $|g_{\sigma\gamma\gamma}/g_{\sigma\pi\pi}|$ for the dispersive and dynamical approaches of sections 2 and 3, respectively. The second and third rows correspond to the dispersive approach with s_σ from ref.[8] and [10], respectively. The result from the dynamical approach are shown in the last row. This approach makes use of strong amplitudes with s_σ very close to that of ref.[80]. Notice that in order to calculate $F_I(s)$, and then $\sigma(\gamma\gamma \rightarrow \pi^0\pi^0)$, s_σ is not needed. The different columns in table 1 represent different contributions to L_I . From left to right in table 1: only the Born term is taken as left hand cut, Born term and vector resonance exchanges, Born term and axial-vector resonance

$ g_{\sigma\gamma\gamma}/g_{\sigma\pi\pi} \times 10^3$	Born	Born + vector	Born + axial	All
Dispersive approach s_σ from ref.[8]	2.60	2.22	2.37	2.01 ± 0.11
Dispersive approach s_σ from ref.[10]	2.42	2.02	2.25	1.85 ± 0.09
Dynamical approach	2.05	1.84	1.81	1.61

Table 1: Different contributions to the ratio $|g_{\sigma\gamma\gamma}/g_{\sigma\pi\pi}|$ given by the dispersive approach of section 2, second and third row, and the dynamical one of section 3, fourth row. In the second row the s_σ pole position is taken from ref.[8], while for the third one s_σ comes from ref.[10]. No error is given for the dynamical approach since this model is very constraint and the systematic uncertainties cannot be worked out.

exchanges and all together. We observe that the interferences between the different pieces has opposite sign to those in the $\gamma\gamma \rightarrow \pi^0\pi^0$ cross section, fig.4. This difference occurs because in the $\pi^0\pi^0$ cross section both the $I = 0$ and $I = 2$ play a role, while in the σ width only the $I = 0$ takes part. For the dispersive results we have taken the average the resulting ratios $|g_{\sigma\gamma\gamma}/g_{\sigma\pi\pi}|$ obtained with PY and CGL parameterizations. The values obtained if using AO agree with the values shown within one sigma. No errorbar is given for the dynamical model result because this model is very constraint, has no free parameters, and the systematic uncertainty cannot be estimated. Its value is quite close to that of the second column, with s_σ from [10], only a 10% lower.

These ratios of residua at the σ pole position are the well defined predictions that follow from our $F_0(s)$, given s_σ . However, the radiative width to $\gamma\gamma$ for a wide resonance like the σ , though more intuitive, has experimental determinations that are parameterization dependent. This is due to the non-trivial interplay between background and the broad resonant signal as stressed in ref.[29]. An unambiguous definition is then required and we employ the standard narrow resonance width formula in terms of $g_{\sigma\gamma\gamma}$ as determined from the residue at s_σ ,

$$\Gamma(\sigma \rightarrow \gamma\gamma) = \frac{|g_{\sigma\gamma\gamma}|^2}{16\pi M_\sigma}, \quad (4.55)$$

as done in refs.[26, 29]. Nevertheless, the determinations of the radiative widths from this expression and those from common experimental analyses of physical data can differ at the level of a $\lesssim 20\%$, as discussed in ref.[29]. Notice that in the equations usually employed in phenomenological fits to data, e.g. see ref.[31], the couplings are determined along the real axis, while the definition eq.(4.55) requires to move to the pole position.

The use of a narrow width resonance formula eq.(4.55) in order to evaluate $\Gamma(\sigma \rightarrow \gamma\gamma)$ is a precise definition and convenient criterion, though somewhat arbitrary as the σ meson has a large width. Elaborating a bit more on this issue let us introduce the normalized σ mass distribution $D(s)$,

$$\int_{4m_\pi^2}^{\infty} D(s)ds = 1. \quad (4.56)$$

Then,

$$\Gamma_{\sigma \rightarrow \gamma\gamma} = \frac{|g_{\sigma\gamma\gamma}|^2}{8\pi M_\sigma} \int_{4m_\pi^2}^{\infty} \frac{q_\gamma}{s^{1/2}} D(s) , \quad (4.57)$$

with $q_\gamma = \sqrt{s}/2$ is the photon center of mass three-momentum. We can then rewrite eq.(4.57) as,

$$\Gamma_{\sigma \rightarrow \gamma\gamma} = \frac{|g_{\sigma\gamma\gamma}|^2}{16\pi M_\sigma} \int_{4m_\pi^2}^{\infty} D(s) ds = \frac{|g_{\sigma\gamma\gamma}|^2}{16\pi M_\sigma} . \quad (4.58)$$

In the last step we have taken into account eq.(4.56). Despite the introduction of the mass distribution for the σ , $D(s)$, eq.(4.58) corresponds to the narrow resonance width approximation due to the null mass of the photons. Of course, in the previous equations we have assumed an energy independent coupling $g_{\sigma\gamma\gamma}$. A more physical calculation would imply to take this dependence into account but this is beyond the scope of the present paper. In the following, we shall content ourselves with eq.(4.55) as a well defined translation from $|g_{\sigma\gamma\gamma}|$ to the more familiar concept of width.

In order to determine $\Gamma(\sigma \rightarrow \gamma\gamma)$ by applying eq.(4.55) with the values given in table 1 one needs to provide numbers for $|g_{\sigma\pi\pi}|$. This is a crucial input to evaluate the width to two photons as the latter is proportional to $|g_{\sigma\pi\pi}|^2$. We first consider the value $|g_{\sigma\pi\pi}^{AO}| = (3.17 \pm 0.10)$ GeV from the approach of ref.[10].^{#7} The calculated width is then

$$\Gamma^{AO}(\sigma \rightarrow \pi\pi) = (1.50 \pm 0.18) \text{ KeV} . \quad (4.59)$$

Not only the position of the pole in the partial wave amplitude, but also its residue can be calculated in the framework of the dispersive analysis described in ref.[8]. Expressed in terms of the complex coefficient $g_{\sigma\pi\pi}$ defined in eq.(4.53), the preliminary result for the residue amounts to $|g_{\sigma\pi\pi}| = (3.31_{-0.08}^{+0.17})$ GeV.^{#8}

$$\Gamma^{CCL}(\sigma \rightarrow \gamma\gamma) = (1.98_{-0.24}^{+0.30}) \text{ KeV} , \quad (4.60)$$

Taking the average between the values in eqs.(4.59) and (4.60) we end with,

$$\Gamma(\sigma \rightarrow \gamma\gamma) = (1.68 \pm 0.15) \text{ KeV} . \quad (4.61)$$

This number is in agreement with the values (1.8 ± 0.4) KeV, with s_σ from ref.[80], and (2.1 ± 0.3) KeV, with s_σ from ref.[8], calculated in ref.[29]. Note that we use here the most recent analysis of ref.[10] instead of ref.[80] for the σ pole position and coupling. In addition, the coupling $|g_{\sigma\pi\pi}^{CCL}|$ has been also explicitly evaluated from ref.[8], which was not known at the time of refs.[26, 29]. On the other hand, eq.(4.61) agrees at the level of one sigma with the estimate $\Gamma(\sigma \rightarrow \gamma\gamma) = (1.2 \pm 0.4)$ KeV of ref.[84], that considers the experimental data on the proton electromagnetic polarizabilities.

Pennington in ref.[26] predicted $\Gamma^{CCL}(\sigma \rightarrow \gamma\gamma) = (4.09 \pm 0.29)$ KeV for s_σ from ref.[8]. The difference between this number and our result in eq.(4.60) is due to i) ref.[26] calculates $|g_{\sigma\gamma\gamma}/g_{\sigma\pi\pi}| = (2.53 \pm 0.09) \times 10^{-3}$ for s_σ from ref.[8] instead of $(2.01 \pm 0.11) \times 10^{-3}$ as given in

^{#7}We thank M. Albaladejo for supplying this number before publication.

^{#8}We express our gratitude to I. Caprini and H. Leutwyler for sending us this result for the residue.

the second row of table 1. This is due to the omission of the axial-vector resonance exchanges in ref.[26, 28], 10%, and to the improvement in our approach by taking into account one extra subtraction and slight different input for the phases, another 10%. One then has the suppression factor $(2.01/2.53)^2 = 0.63$ for the width $\Gamma(\sigma \rightarrow \gamma\gamma)$. ii) There is also the difference with regards the value of the $|g_{\sigma\pi\pi}^{CCL}|$ employed. Ref.[26] uses $|g_{\sigma\pi\pi}^{CCL}| = 3.86$ GeV instead of 3.3 GeV, with the last number very close to our previous estimate of $|g_{\sigma\pi\pi}^{CCL}|$ in ref.[29] (see eq.(3.14) of this reference). The additional suppression factor $(3.3/3.86)^2 = 0.73$ then raises. iii) Finally, ref.[26] includes and extra factor $|\beta(s_\sigma)| = 0.956$ as compared with eq.(4.55). Taking all these several factors into account one has $4.09 \text{ KeV} \rightarrow 4.09 \times 0.63 \times 0.73 \times 1.05 = 1.98 \text{ KeV}$, as in eq.(4.60).

As it is stressed in ref.[26], the σ resonance is far from dominating the $\gamma\gamma \rightarrow \pi^0\pi^0$ reaction. Were this the case, then

$$F_N(s) \simeq \frac{g_{\sigma\pi^0\pi^0}g_{\sigma\gamma\gamma}}{s_\sigma - s}, \quad (4.62)$$

from where

$$\sigma(\gamma\gamma \rightarrow \pi^0\pi^0) \simeq \frac{8\pi}{3M_\sigma^2} \frac{\Gamma(\sigma \rightarrow \gamma\gamma)}{\Gamma(\sigma \rightarrow \pi\pi)}. \quad (4.63)$$

Given the value of $\sigma(\gamma\gamma \rightarrow \pi^0\pi^0) \simeq 16 \text{ nb}$ in the peak, one then concludes that the $\Gamma(\sigma \rightarrow \gamma\gamma) \simeq 0.39 \text{ KeV}$, which is about a factor 4 smaller than our calculation eq.(4.61), and one order of magnitude smaller than the value of ref.[26]. In this latter reference it was argued that the reason for this difference is the very strong destructive interference between the $I = 2$ and $I = 0$ amplitudes, see fig.5. However, a quantitative analysis, like that offered in ref.[26], is affected by the fact that the ratio $|F_0/F_N|^2$ depends strongly on the precise energy where it is evaluated in the energy region where $\gamma\gamma \rightarrow \pi^0\pi^0$ peaks. This is clearly seen in fig.5. At 400 MeV the ratio $|F_0/F_N|^2 \simeq 12$ (one has to multiply by 3 the ratio of the cross sections of $I = 0$ and $\pi^0\pi^0$ to correct for the Clebsch-Gordan coefficient in eq.(3.31)), while at 500 MeV is $\sim 3/2$. This figure also shows that peak of the $\gamma\gamma \rightarrow \pi^0\pi^0$ cross section at around 500 MeV is not directly related to the σ resonance, but a result of the strong interference between the $I = 2$ and $I = 0$ components. Note also that the latter lacks of a resonance structure around the σ due to the Adler zero in $F_N(s)$.^{#9} The σ resonance, present in the $I = 0$ component, distorts the form of the $I = 0$ Born term accumulating strength towards the threshold so that above $\sqrt{s} \sim 0.5 \text{ GeV}$ $|F_0(s)|$ is much smaller than the $I = 2$ counterpart.

5 Conclusions

We have performed a theoretical study of the reaction $\gamma\gamma \rightarrow \pi^0\pi^0$ making use of improved versions of the approaches of refs.[29] and [19]. The former is based on a dispersion relation for $\gamma\gamma \rightarrow \pi\pi$ in S-wave and definite isospin I similar to that of refs.[26–28], but including one more subtraction for $I = 0$. This constant is fixed by taking into account an additional constraint based on a lax bound for the size of the $f_0(980)$ peak in $\gamma\gamma \rightarrow \pi^0\pi^0$ or, equivalently, for the value of $\Gamma(f_0(980) \rightarrow \gamma\gamma)$ from ref.[31]. In this way, ref.[29] was able to drastically reduce the uncertainty in the results of ref.[26] on the function phase $\phi_0(s')$ of $F_0(s)$ taken above the $K\bar{K}$ threshold. Here, we have

^{#9}See refs.[73, 85] for a discussion on the role of the Adler zeroes and σ resonant shapes in two pion production processes.

been able to reduce it further so that it is shown that $\phi_0(s)$ should follow quite closely $\delta_0(s)$ above the $K\bar{K}$ threshold. Then, in the advent of better experimental data on $\sigma(\gamma\gamma \rightarrow \pi^0\pi^0)$, our present results allow a sharper comparison with data in order to distinguish between different parameterizations for the low energy $\pi\pi$ $I = 0$ S-wave.

We have also updated the approach of ref.[19] adding the crossed exchanges of the K^* and the nonet of the lightest 1^{++} axial-vector resonances, not included in this reference. The axial-vector exchanges of the 1^{+-} and 1^{++} resonances were not either taken into account in ref.[26, 28], but have been included here. The explicit expressions and calculation details for the different elements both in the dispersive and dynamical approaches are also given. In particular, the expressions for the Born terms and the crossed exchanges of the 1^{--} , 1^{+-} and 1^{++} vector and axial-vector resonances, respectively, are collected.

The role of the σ and $f_0(980)$ resonances in $\gamma\gamma \rightarrow \pi\pi$ has been also addressed. For the latter resonance it was argued by continuity arguments that it should come up as a small peak, as actually seen recently in ref.[31] for $\gamma\gamma \rightarrow \pi^+\pi^-$. Importantly, the fact that it is indeed a peak requires that the phase of $F_0(s)$ should rapidly increased around the $K\bar{K}$ threshold, the so called $z = +1$ scenario. Regarding the σ resonance, we have calculated the ratio of the residua $|g_{\sigma\gamma\gamma}/g_{\sigma\pi\pi}| = 1.91 \pm 0.07$ taking into account the values of the σ pole position, s_σ , of refs.[8, 10]. One should stress that the calculation of $\sigma(\gamma\gamma \rightarrow \pi\pi)$ is independent of the value taken for s_σ and $|g_{\sigma\pi\pi}|$, though they are essential inputs for calculating the width $\Gamma(\sigma \rightarrow \gamma\gamma)$. With $|g_{\sigma\pi\pi}^{AO}| = (3.17 \pm 0.10)$ GeV for s_σ of ref.[10] one has $\Gamma^{AO}(\sigma \rightarrow \gamma\gamma) = (1.50 \pm 0.18)$ KeV and with $|g_{\sigma\pi\pi}^{CCL}| = (3.31_{-0.08}^{+0.17})$ GeV, a preliminary value corresponding to the s_σ of ref.[8], $\Gamma^{CCL}(\sigma \rightarrow \gamma\gamma) = (1.98_{-0.24}^{+0.30})$ KeV. The average between the previous two values reads $\Gamma(\sigma \rightarrow \gamma\gamma) = (1.68 \pm 0.15)$ KeV, that we take as our final result for the width.

Acknowledgements

We thank Carlos Schat for fruitful discussions and collaboration in this research and in ref.[29] during his stay in the Physics Department of the University of Murcia. This work has been supported in part by the MEC (Spain) and FEDER (EC) Grants FPA2004-03470, FPA2007-62777 and Fis2006-03438, the Fundación Séneca (Murcia) grant Ref. 02975/PI/05, the European Commission (EC) RTN Network EURIDICE under Contract No. HPRN-CT2002-00311 and the HadronPhysics I3 Project (EC) Contract No RII3-CT-2004-506078.

References

- [1] J. A. Oller and E. Oset, Nucl. Phys. **A620**, 438 (1997); (E)-ibid. **A652** (1999) 407].
- [2] J. A. Oller and E. Oset, Phys. Rev. **D60**, 074023 (1999).
- [3] A. Dobado and J. R. Peláez, Phys. Rev. **D56**, 3057 (1997); J. A. Oller, E. Oset and J. R. Peláez, Phys. Rev. Lett. **80**, 3452 (1998); J. A. Oller, E. Oset and J. R. Peláez, Phys. Rev. **D59**, 074001 (1999) (E)-ibid. **D60**, 099906 (1999), **D75**, 099903 (2007).
- [4] J. R. Peláez, Phys. Rev. Lett. **92**, 102001 (2004); J. R. Peláez and G. Rios, Phys. Rev. Lett. **97**, 242002 (2006).

- [5] T. Hannah, Phys. Rev. D **60**, 017502 (1999).
- [6] S. Weinberg, Physica **A96**, 327 (1979).
- [7] J. Gasser and H. Leutwyler, Ann. Phys. (N.Y.) **158**, 142 (1984); Nucl. Phys. **B250**, 465 (1985).
- [8] I. Caprini, G. Colangelo and H. Leutwyler, Phys. Rev. Lett. **96** (2006) 132001.
- [9] F. J. Ynduráin, R. Garcí-Martín and J. R. Peláez, arXiv:hep-ph/0701025.
- [10] M. Albaladejo and J. A. Oller, arXiv:0801.4929 [hep-ph]; arXiv:0711.1977 [hep-ph].
- [11] J. Bijnens and F. Cornet, Nucl. Phys. **B296**, 557 (1988).
- [12] J. F. Donoghue, B. R. Holstein and Y. C. Lin, Phys. Rev. **D37**, 2423 (1988).
- [13] H. Marsiske *et al.* [Crystal Ball Collaboration], Phys. Rev. **D41**, 3324 (1990).
- [14] S. Bellucci, J. Gasser and M. E. Sainio, Nucl. Phys. **B423**, 80 (1994).
- [15] J. Gasser, M. A. Ivanov and M. E. Sainio, Nucl. Phys. **B728**, 31 (2005).
- [16] G. Ecker, J. Gasser, A. Pich and E. de Rafael, Nucl. Phys. **B321** (1989) 311; G. Ecker, J. Gasser, H. Leutwyler, A. Pich and E. de Rafael, Phys. Lett. **B223** (1989) 425.
- [17] A. Dobado and J. R. Peláez, Z. Phys. **C57**, 501 (1993).
- [18] J. F. Donoghue and B. Holstein, Phys. Rev. **D48**, 137 (1993).
- [19] J. A. Oller and E. Oset, Nucl. Phys. **A629**, 739 (1998).
- [20] J. A. Oller, Phys. Lett. **B426**, 7 (1998).
- [21] T. S. H. Lee, J. A. Oller, E. Oset and A. Ramos, Nucl. Phys. **A643** (1998) 402.
- [22] U. G. Meissner and J. A. Oller, Nucl. Phys. A **679**, 671 (2001).
- [23] J. A. Oller, E. Oset and J. E. Palomar, Phys. Rev. **D63** (2001) 114009.
- [24] E. Oset, J. A. Oller and U. G. Meissner, Eur. Phys. J. **A12**, 435 (2001).
- [25] E. Oset, J. R. Peláez and L. Roca, Phys. Rev. **D67**, 073013 (2003); arXiv:0801.2633 [hep-ph].
- [26] M. R. Pennington, Phys. Rev. Lett. **97** (2006) 011601.
- [27] D. Morgan and M. R. Pennington, Z. Phys. **C37**, 431 (1988); (E)-*ibid.* **C39**, 590 (1988); Phys. Lett. **B272**, 134 (1991).
- [28] M. R. Pennington, pag.18 in L. Maiani, G. Panchieri and N. Paver, eds., The DAΦNE Physics Handbook (INFN, Frascati, 1992).
- [29] J. A. Oller, L. Roca and C. Schat, Phys. Lett. **B659**, 201 (2008).
- [30] J. A. Oller and L. Roca, Phys. Lett. **B651**, 139 (2007); J. A. Oller, L. Roca and C. Schat, arXiv:0711.2125 [hep-ph].
- [31] T. Mori *et al.* [Belle Collaboration], Phys. Rev. **D75** (2007) 051101.
- [32] J. Babcock and J. L. Rosner, Phys. Rev. **D14** (1976) 1286.
- [33] S. Godfrey and N. Isgur, Phys. Rev. **D32** (1985) 189.
- [34] T. Barnes, Phys. Lett. **B165**, 434 (1985).

- [35] M. S. Chanowitz, *Proceedings of the VIth International Workshop on Photon-Photon Collisions, Lake Tahoe*, edited by U. Karshon (World Scientific, Singapore, 1988) p.205.
- [36] S. Narison and G. Veneziano, *Int. J. Mod. Phys.* **A4** (1989) 2751.
- [37] Z. P. Li, F. E. Close and T. Barnes, *Phys. Rev.* **D43** (1991) 2161.
- [38] C. R. Munz, *Nucl. Phys.* **A609** (1996) 364.
- [39] N. N. Achasov, *Phys. Atom. Nucl.* **65** (2002) 546 [*Yad. Fiz.* **65**, 573 (2002)].
- [40] S. Krewald, R. H. Lemmer and F. P. Sassen, *Phys. Rev. D* **69** (2004) 016003.
- [41] S. Rodriguez and M. Napsuciale, *Phys. Rev.* **D71**, 074008 (2005).
- [42] C. Hanhart, Yu. S. Kalashnikova, A. E. Kudryavtsev and A. V. Nefediev, *Phys. Rev.* **D75** (2007) 074015.
- [43] G. Mennessier, P. Minkowski, S. Narison and W. Ochs, arXiv:hep-ph/0707.4511.
- [44] F. J. Ynduráin, *Phys. Lett.* **B578**, 99 (2004); (E)-*ibid* **B586**, 439 (2004).
- [45] F. J. Ynduráin, *Phys. Lett.* **B612**, 245 (2005).
- [46] F. J. Ynduráin, arXiv:hep-ph/0510317.
- [47] B. Ananthanarayan, I. Caprini, G. Colangelo, J. Gasser and H. Leutwyler, *Phys. Lett.* **B602**, 218 (2004).
- [48] J. F. Donoghue, J. Gasser and H. Leutwyler, *Nucl. Phys.* **B343**, 341 (1990).
- [49] B. Moussallam, *Eur. Phys. J.* **C14**, 111 (2000).
- [50] U. G. Meißner and J. A. Oller, *Nucl. Phys.* **A679**, 671 (2001).
- [51] F. E. Low, *Phys. Rev.* **96**, 1428 (1954); M. Gell-Mann and M. L. Goldberger, *Phys. Rev.* **96**, 1433 (1954).
- [52] B. Hyams *et al.*, *Nucl. Phys.* **B64**, 134 (1973).
- [53] G. Grayer *et al.*, *Nucl. Phys. B* **75** (1974) 189.
- [54] R. Kaminski, L. Lesniak and K. Rybicki, *Z. Phys. C* **74**, 79 (1997).
- [55] S Pislak *et al.* [BNL-E865 Collaboration], *Phys. Rev. Lett.* **87**, 221801; *Phys. Rev.* **D67**, 072004 (2003).
- [56] L. Masetti [NA48/2 Collaboration], arXiv:hep-ex/0610071.
- [57] M. J. Losty *et al.*, *Nucl. Phys.* **B69** (1974) 185.
- [58] W. Hoogland *et al.*, *Nucl. Phys.* **B126** (1977) 109.
- [59] G. Colangelo, J. Gasser and H. Leutwyler, *Nucl. Phys.* **B603**, 125 (2001).
- [60] J. R. Peláez and F. J. Ynduráin, *Phys. Rev.* **D68**, 074005 (2003); *Phys. Rev.* **D71**, 074016 (2005).
- [61] N. N. Achasov, *Proceedings of the 14th International Seminar on High Energy Physics: Quarks 2006, St. Petersburg, Russia*.
- [62] G. Mennessier, *Z. Phys.* **C16**, 241 (1983).

- [63] W. Wetzel *et al.*, Nucl. Phys. **B115**, 208 (1976); V. A. Polychromatos *et al.*, Phys. Rev. **D19**, 1317 (1979); D. Cohen *et al.* Phys. Rev. **D22**, 2595 (1980); E. Etkin *et al.*, Phys. Rev. **D25**, 1786 (1982).
- [64] Pyungwon Ko, Phys. Rev. **D41**, 1531 (1990).
- [65] J. F. Donoghue, B. Holstein and D. Wyler, Phys. Rev. **D47**, 2089 (1993).
- [66] S. Weinberg, Phys. Rev. Lett. **18** (1967) 507.
- [67] K. Kawarabayashi and M. Suzuki, Phys. Rev. Lett. **16**, 255 (1966); Riazuddin and Fayyazuddin, Phys. Rev. **147**, (1966) 1071.
- [68] J. Prades, Z. Phys. **C63**, 491 (1994); (E)-*ibid.* **C11**, 571 (1999).
- [69] J. Bijnens, C. Bruno and E. de Rafael, Nucl. Phys. **B390**, 501 (1993).
- [70] W.-M. Yao *et al.*, Journal of Physics **G33**, 1 (2006).
- [71] M. R. Pennington, T. Mori, S. Uehara and Y. Watanabe, arXiv:0803.3389 [hep-ph].
- [72] L. Roca, J. E. Palomar, E. Oset and H. C. Chiang, Nucl. Phys. **A744**, 127 (2004); AIP Conf. Proc. **814**, 634 (2006).
- [73] J. A. Oller, Phys. Rev. **D71**, 054030 (2005).
- [74] J. A. Oller, Nucl. Phys. **A714**, 161 (2003); J. E. Palomar, L. Roca, E. Oset and M. J. Vicente Vacas, Nucl. Phys. **A729**, 743 (2003). E. Marco, S. Hirenzaki, E. Oset and H. Toki, Phys. Lett. **B470**, 20 (1999);
- [75] S. Weinberg, Phys. Lett. **B251** (1990) 288; Nucl. Phys. **B363** (1991) 3.
- [76] E. Epelbaum, W. Gloeckle and U. G. Meissner, Nucl. Phys. **A637** (1998) 107; Nucl. Phys. **A671** (2000) 295.
- [77] D. R. Entem and R. Machleidt, Phys. Rev. **C68** (2003) 041001; S. K. Bogner, T. T. S. Kuo, A. Schwenk, D. R. Entem and R. Machleidt, Phys. Lett. **B576** (2003) 265.
- [78] E. Oset, H. Toki, M. Mizobe and T. T. Takahashi, Prog. Theor. Phys. **103** (2000) 351.
- [79] J. Schwinger, Ann. Phys. **2**, 407 (1957); M. Gell-Mann and M. Levy, Nuovo. Cim. **XVI**, 705 (1960); B. W. Lee, Nucl. Phys. **B9**, 649 (1969); S. Gasiorowicz and D. A. Geffen, R. J. Schecter and Y. Ueda, Phys. Rev. **D3**, 2874 (1971);(E)-*ibid.* **D8**, 987 (1973); H. Pagels, Phys. Rept. **C16**, 219 (1975); N. A. Törnqvist, Eur. Phys. J. **C11**, 359 (1999).
- [80] J. A. Oller, Nucl. Phys. **A727** (2003) 353.
- [81] J. A. Oller, proceedings of the Workshop “Possible Existence of the σ -meson and its implications to Hadron Physics, KEK Proceedings 2000-4, NUP B-2000-1, 33; Soryushiron Kenkyu **102**, 33 (2001); arXiv:hep-ph/0007349.
- [82] S. Weinberg, “*The Quantum theory of fields. Vol. 1: Foundations*”, Cambridge University Press (1995).
- [83] U. G. Meissner, Phys. Rept. **161**, 213 (1988).
- [84] J. Bernabéu and J. Prades, arXiv:0802.1830 [hep-ph].
- [85] J. A. Oller, *In the Proceedings of 2nd Workshop on the CKM Unitarity Triangle, Durham, England, 5-9 Apr 2003, pp WG412* [arXiv:hep-ph/0306294].